Schweiz. Z. Hydrol. 40/1, 1978, Birkhäuser Verlag Basel

On the gravitational seiches of Lake Constance and their generation

By Paul F. Hamblin[1]) and Eckard Hollan[2])
1) Canada Centre for Inland Waters, Burlington, Ontario, Canada
2) Institute for Environmental Protection of the State of Baden-Württemberg, West Germany (Landesanstalt für Umweltschutz Baden-Württemberg, BRD)

Manuscript received on 10 January 1978

ABSTRACT

Although the surface seiches of Lake Constance have been observed as early as 1549 and received serious scientific attention since 1893 in the classical work of Forel, they have only recently been investigated by modern hydrodynamical methods. It is the goal of this report to critically compare theoretical predictions of the periods and form of seiches with recent and historical observations as well as to examine the mechanisms of generation of these surface oscillations by means of applying measured atmospheric forcing in Lake Constance to a theoretical model. In the first part of this work, we review the findings of a large number of previous investigations, while the second part consists of a verification analysis of the model predictions of seiches. In the final part, we present a theory, predictions and observations of the excitation of seiches by arbitrary wind and barometric pressure gradient forcing.

1. Previous findings on the seiches of Lake Constance

The first report on seiches of Lake Constance stems from the chronicler, Christoph Schulthaiss [15], who describes an oscillation of the lake at the city of Constance on 23 February 1549 with a wave height of about 60 cm and a period between 12 and 15 minutes. As a result of our computations, this remarkable seiche case has been identified as a higher mode of seiche of Lake Constance in resonance with the fundamental oscillation of the Bay of Konstanz (see fig. 11).
The first systematic investigation was undertaken by Forel [1] in the years 1874, 1890 and 1891. He determined the periods of the first three and some higher modes (table 1). Since the spatial resolution of his observations was not sufficient, the second and third mode were not identified correctly. Due to a misinterpretation of the observed periods by Merian's formula as it turned out from our computations, Forel considered the third mode as the second, and left the latter one unexplained.
After Forel's study, the seiches were observed frequently in Konstanz and Bregenz. Gasser [3] evaluated the records between 1931 and 1939 from Bregenz and those from Konstanz between 1913 and 1950 with respect to the weather conditions prevailing during the occurrence of seiches. He concluded that pressure changes as

well as strong and local winds may cause the oscillations and gave a frequency distribution of higher seiches and of their damping rate throughout the year.
A thorough investigation of the seiches and their generating forces was then undertaken from 1966 through 1973 by Mühleisen and Kurth [10]. In this programme, the seiches were observed at 10 stations, the windfield at up to 16 stations on the shore, and the air pressure by microbarographs at up to 5 stations. The wind was also observed over the lake on board the ferry Friedrichshafen-Romanshorn (fig. 11). It is this observational material which underlies the following investigation of the seiches of Lake Constance.
In a first attempt, Mühleisen and Fischer [9] used this material and treated the excitation of seiches by air pressure changes in a rectangular model of the lake. The results show that a satisfactory explanation is only possible when a two-dimensional theory is applied which accounts for the generation by pressure gradients as well as variable wind stress.

2. The seiches of Lake Constance

2.1 *Theoretical model*

The equations governing the dynamics of surface seiches are the shallow-water equations for a homogeneous fluid on a plane of constant rotation. Let the vertically averaged velocity have components, u and v, in the east and north direction and the fluid have an equilibrium depth of h. Letting g denote the acceleration of gravity and f the local Coriolis parameter, then our mathematical description of seiches may be written as,

$$\frac{\partial u}{\partial t} - fv + g\frac{\partial \eta}{\partial x} = 0,$$

$$\frac{\partial v}{\partial t} + fu + g\frac{\partial \eta}{\partial y} = 0,$$

$$\frac{\partial \eta}{\partial t} + \frac{\partial (hu)}{\partial x} + \frac{\partial (hv)}{\partial y} = 0.$$

In the above equations, the free surface displacement is denoted by η and the frictional and non-linear terms are neglected. Since we seek periodic solutions, it is convenient to assume that the dependent variable have an exponential time dependence of frequency σ.
It is straightforward to derive an appropriate variational formulation of the above equations for all boundary conditions requiring zero energy flux across the boundaries. In this case, we may write the functional, I, as

$$I(\eta) = \iint_A \left[\eta\eta^* + \frac{gh}{f^2-\sigma^2}\left\{\frac{f}{i\sigma}\left(\frac{\partial \eta}{\partial y}\frac{\partial \eta^*}{\partial x} - \frac{\partial \eta}{\partial x}\frac{\partial \eta^*}{\partial y}\right) + \frac{\partial \eta}{\partial x}\frac{\partial \eta^*}{\partial x} + \frac{\partial \eta}{\partial y}\frac{\partial \eta^*}{\partial y}\right\}\right] dx\,dy$$

where the asterisk denotes the complex conjugate of the complex free surface variable, η, and i is the square root of minus one.
Implicit in the boundary condition of zero radiation of energy across the boundaries are the usual dynamical conditions namely: 1. zero depth at the shoreline and finite η and its gradients; 2. finite depth at the boundary but vanishing normal velocity; 3. finite depth and normal velocity but zero free surface displacement along the boundary. In Lake Constance conditions 1 and 2 apply.
Physically, the quadratic form represents the total kinetic and potential energy within the lake associated with the free oscillations. The solution of our variational problem is the function that minimizes the functional. The essence of the numerical procedure adopted here is that an approximation to the quadratic form is first obtained by partitioning the lake into a series of small zones or elements, representing the solution in each element by a polynomial of the second degree, performing the integrations piecewise in each element and finally after the summation of contributions from all elements is taken, the minimum of the approximate functional is found.
If the variables, η and η^*, are represented locally by Lagrangian interpolation functions, ψ, then the unknowns at certain points in each element which will be referred to as nodal points become the weighting coefficients, $\dot{q}_k$, as follows.

$$\eta = \sum_k \dot{q}_k \psi_k .$$

Substitution of the above definition into the functional yields a system of 6 equations for each element

$$\sum_{j=1}^{6} \iint \left[\psi_k \psi_j + \frac{gh}{f^2 - \sigma^2} \left\{ \frac{f}{i\sigma} \left(\frac{\partial \psi_k}{\partial y} \frac{\partial \psi_j}{\partial x} - \frac{\partial \psi_k}{\partial x} \frac{\partial \psi_j}{\partial y} \right) + \frac{\partial \psi_k}{\partial x} \frac{\partial \psi_j}{\partial x} + \frac{\partial \psi_k}{\partial y} \frac{\partial \psi_j}{\partial y} \right\} \right] \dot{q}_k \dot{q}_j^* \, dx \, dy = I_k$$

$$k = 1, \ldots, 6 .$$

The equations for the entire lake are obtained by successive integrations of each element and by addition of the resulting equations.
When the appropriate integrations are performed on the basis of the approximation to the free surface, the functional becomes in terms of the unknown free surface displacements $\dot{q}$ and $\dot{q}^*$ at each node

$$I(\dot{q}, \dot{q}^*) = \dot{q}^{*T} \sigma^3 [L] \dot{q} + \dot{q}^{*T} \sigma [M] \dot{q} + \dot{q}^{*T} [N] \dot{q} .$$

The vectors $\dot{q}$ and $\dot{q}^*$ are the undetermined displacements at each node and the Hermetian matrices L, M and N have been introduced for convenience.

Taking the minimum with respect to $\dot{q}^*$, we obtain

$$\frac{\partial I}{\partial \dot{q}^*} = 0$$

or

$$\sigma^3 [L]\dot{q} + \sigma [M]\dot{q} + [N]\dot{q} = 0$$

where $\dot{q}$ is now the vector of displacement minimizing I.
The problem has been reduced to an algebraic eigenvalue problem of the non-linear or lambda-matrix type. The details of the solution of this problem by the method of generalized Rayleigh quotient iteration are given by Hamblin [4].
A brief outline of the method used to partition the lake into elements is in order. Lake Constance was divided into 98 triangles with straight sides in the interior region and with curved sides adjacent to the lake shoreline as shown in figure 1. The triangularization was performed manually to ensure finer resolution in the areas of interest such as the Bays of Bregenz and Konstanz. In each element the aforementioned nodal points are specified to be the vertices and the three mid-

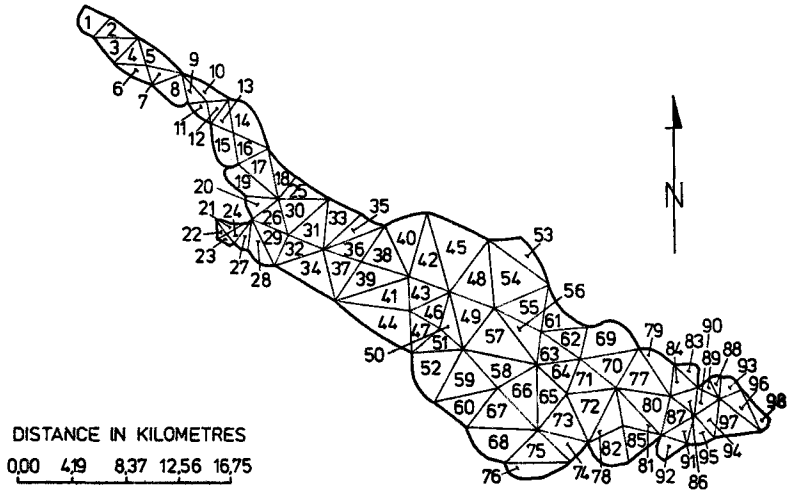

Figure 1. Triangularization of Lake Constance into 98 elements.

edge points, figure 2a. Figure 2b demonstrates that the edge point along a boundary is allowed to coincide with the shoreline.
All integrations arising from the functional expression can be performed analytically save for the boundary elements when a coordinate transformation mapping the curved edge into a straight side requires that numerical methods of integration be employed.
It is noteworthy that the depth variable, h, in the functional is also expanded in an identical polynomial expression in each element when the weighting coefficients

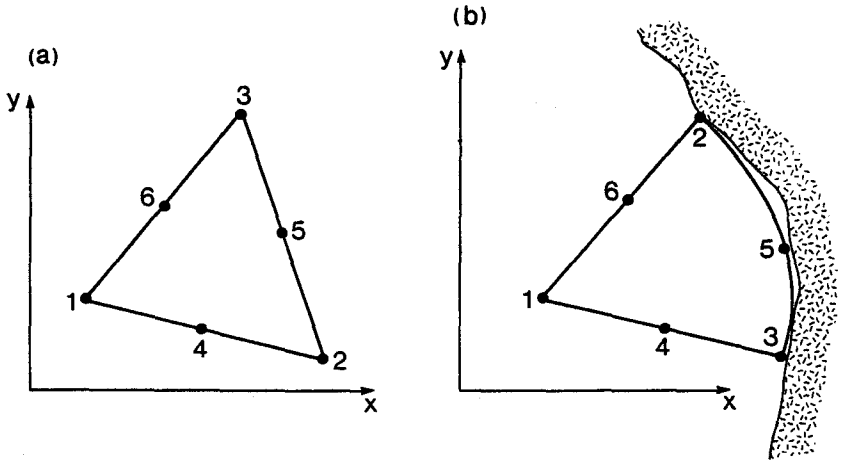

Figure 2. a) Triangular element in the interior of the lake. The six nodes defining the element are numbered. b) Element adjacent to a boundary.

become the specified depths at the six nodes of the triangle. Depths were scaled from the bathymetric chart for Lake Constance published by Graf Zeppelin [18] and updated by the Cartographical Survey of Baden-Württemberg (1968), scale 1 to 5×10^4. The outlines of the bathymetry are depicted in figure 11. Finally, before the computations could be started, the Coriolis parameter was prescribed a constant value appropriate to a central latitude of Lake Constance of 48° N.

2.2 *Model results*

The lowest 11 gravitational seiches have been computed by the method described above. The theoretically determined periods are summarized in table 1. Because of

Table 1. Theoretically predicted and observed periods in minutes of the lowest 11 gravitational seiches. Mixed type refers to both longitudinal and transverse motions. Modes with large amplitudes in Konstanz Bay are indicated.

Mode	Type	Theoretical period (min)	Observed period (min)
1	Longitudinal	53.4	55.5 (25 June 1967)
2	Longitudinal	35.7	38.6 (12 November 1969)
3	Longitudinal	27.2	28.1 (20 July 1967)
4	Longitudinal	19.4	
5	5th mixed	18.6	
6	5th longitudinal	16.4	
7	Mixed	14.8	15[2])
8	Mixed, Constance Bay	14.3	14.6[1])[3])
9	Mixed	12.5	
10	Mixed, Constance Bay	12.0	[3])
11	Mixed	11.3	11.6[1])

1) Fischer [9]. 2) Forel [1]. 3) Schulthaiss [15].

the volume of material involved only the most important directly observed solutions are presented here. A data report is in preparation which lists all computed free surface distributions and the associated current fields [7].
The method of presentation of the spatial distributions of the seiche solutions is somewhat condensed. The free surface displacement at any point in the lake and at any time during an oscillatory cycle may be computed from the plotted amplitude distribution, $A(x,y)$, and the distribution of phase, $\phi(x,y)$, in figures 3–7 according to the expression

$$\eta(x,y,t) = A(x,y)\cos(\sigma t + \phi(x,y)) .$$

The free surface distributions are normalized to a maximum free surface displacement of 100 units.
The calculated periods range from 54 to 11 minutes. In the case of the lowest four gravitational modes, the sense of the rotation of high water around points of zero displacement known as amphidromic points is in the direction of rotation. In the fifth and higher modes, the distribution of phase is more complex with cells rotating in both directions comprising the solutions, for example, the case of the eighth mode, figure 7, where the open circle represents a progression of phase in the clockwise direction. This solution also demonstrates as does the tenth mode the resonance of water in the Bay of Konstanz.

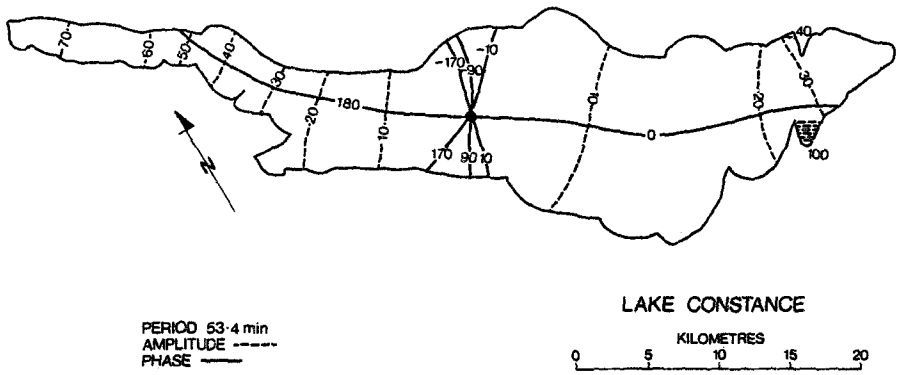

Figure 3. Phase (———) and amplitude (- - - -) distribution of the free surface of the lowest mode, period 53.4 minutes.

A representative example of the associated seiche currents is shown in figure 8 for the fundamental seiche. There it may be evident that when the water level is high at the ends of the lake, the flow is zero and that the flow is maximum when the water level displacement is least. Westerly currents are found when the high water is along the southern shore of the lake. It is unlikely that seiche currents are to be found in conventional current meter recordings since for a typically large seiche amplitude of 10 cm maximum currents are only about 1 cm/s. For this reason, currents are not discussed further.

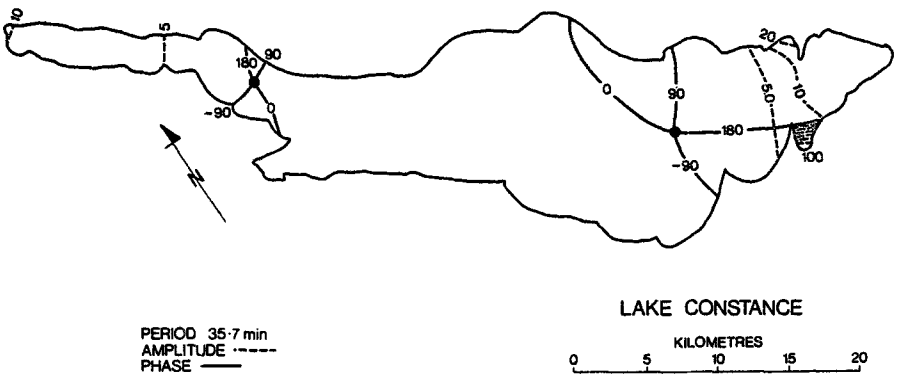

Figure 4. Phase (———) and amplitude (- - - -) distribution of the free surface of the second mode, period 35.7 minutes.

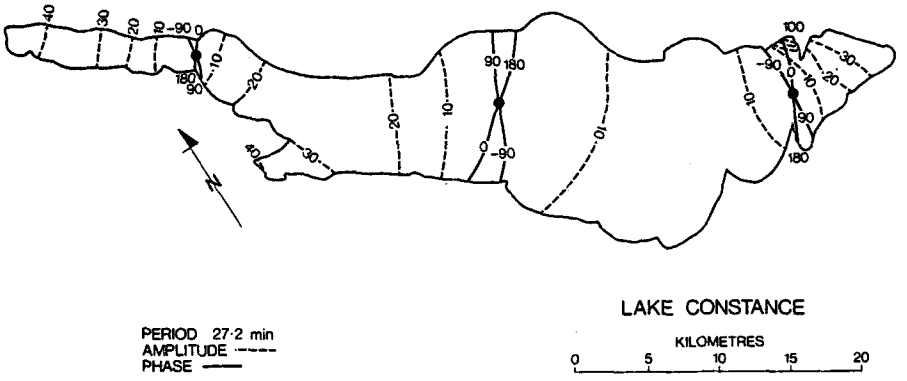

Figure 5. Phase (———) and amplitude (- - - -) distribution of the free surface of the third mode, period 27.2 minutes.

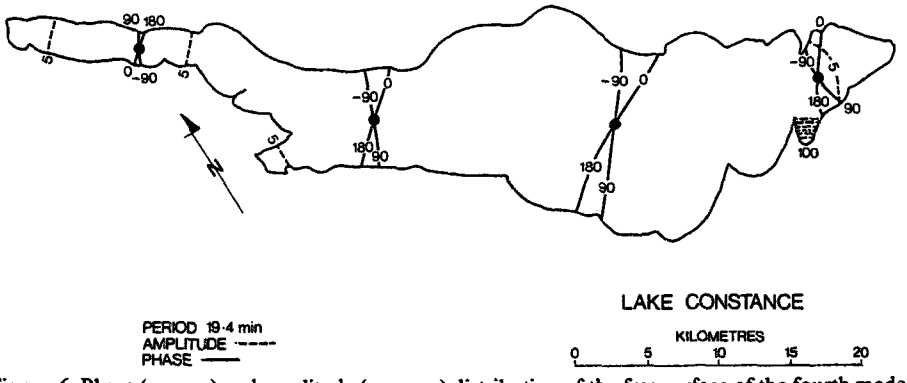

Figure. 6. Phase (———) and amplitude (- - - -) distribution of the free surface of the fourth mode, period 19.4 minutes.

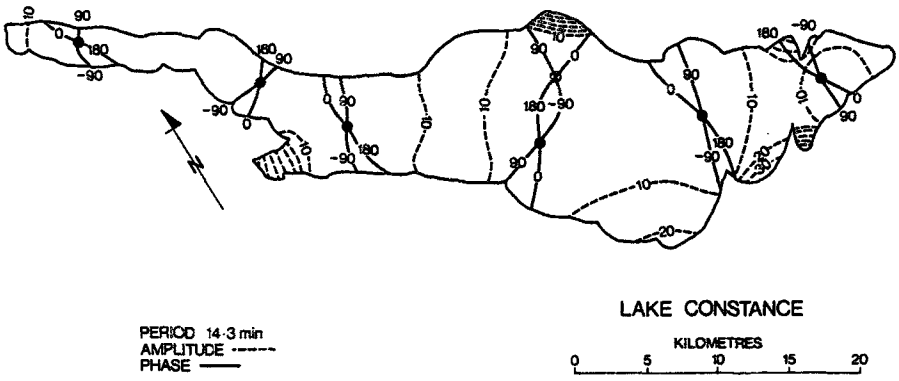

Figure 7. Phase (———) and amplitude (- - - -) distribution of the free surface of the eighth mode, period 14.3 minutes. The open circle denotes advance of phase in the clockwise sense.

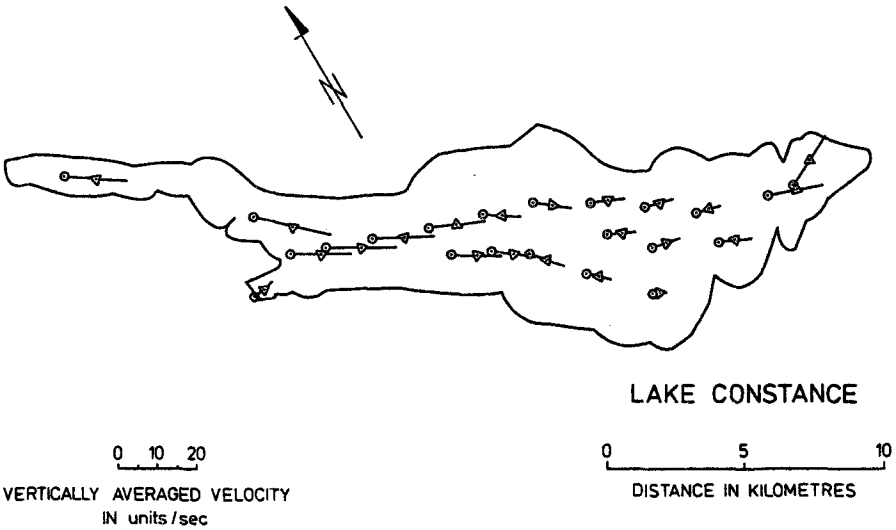

Figure 8. Velocity distribution associated with the fundamental seiche. Solid line means major axis of the current ellipse. The dots in the triangles, and circles represent the position of the flow vector at $\sigma t = 0$ and $\sigma t = \pi/2$, respectively, with respect to an origin located at the mid point of the major axis.

2.3 *Model verification*

In an extensive programme of investigation during the years from 1967 to 1970, a network of 10 water level gauges was established around Lake Constance which is illustrated in figure 11. Several gauges operated until 1973. From a visual inspection of the analogue records at these stations, we selected approximately one dozen cases when seiches were clearly in evidence. It is these data which have been employed for the purpose of model verification.

As will be evident in figures 12–14, seiches are exhibited remarkably clearly compared to other lakes. Therefore, analysis of the records was done by direct inspection rather than by such statistical methods as spectral analysis.

The period of the fundamental seiche was observed to be 55.6 minutes on a particularly clear example on 25 June 1967, which is in agreement with the earlier published results of Forel. The discrepancy of 4% between the observed and computed periods may not be explained by water level differences between the chart depths and the actual depth at the time of measurements. A difference of 1.3 m existed at this time which would account for only a 0.42% correction. It is more likely that the neglect of friction and non-linear effects may account for this difference.

By the use of six episodes in which the fundamental seiche is excited predominantly, we have attempted to verify the amplitude and phase distribution. The amplitudes occurring at simultaneous times were scaled directly from the analogue charts and then normalized by the amplitude at Ludwigshafen. The theoretical and observed distributions are listed in table 2. By careful attention to timing marks on the individual records, the timing of seiche events relative to the Ludwigshafen gauge was evaluated to an estimated resolution of ± 5 minutes.

With the possible exception of the Lindau gauge, the observed distribution of amplitude on the average conforms remarkably closely to the predicted free surface amplitude. It is immediately apparent from the theoretical phase distributions that it is impossible to detect the sense of rotation of the fundamental seiche from the established network of stations and from the timing resolution of ± 5 minutes. However, the general features of phase, that is, whether a station is approximately in phase or 180° out of phase, may readily be established with the possible exception of the Friedrichshafen record. At that location, the phase appears to be opposite to that predicted.

The binodal seiche is rarely exhibited in the lake. In only one instance, 12 November 1969, did we find a distinct example at the Hard station. An average of 10 successive oscillations yielded an estimated period of 38.6 minutes which compares with the theoretical period of 35.7 minutes. It is probable that the period may be somewhat lower than 38.6 minutes. Mühleisen and Fischer [9] have observed 37.5 minutes which is in closer agreement with the predicted values.

The trinodal seiche is exited more frequently than the binodal case. We obtained a period of 28.1 minutes from the cases of 20 July 1967 and 18 June 1969 which compares closely with Fischer's result of 28.0 and the theoretical result of 27.2 minutes. It is possible to estimate certain features of the amplitude distribution of the third mode. At the stations Konstanz-Jakobsbad, Hagnau and Langenargen, the amplitudes are in the ratios 5:3:2.5 compared to the theoretical ratios of 5:2.5:1.3. The in-phase agreement between Konstanz and Hagnau has been confirmed in the two episodes whereas the phase at Langenargen does not appear to fit the predicted distribution.

Seiches of higher orders are seldom clearly exhibited in the records except for the case of the eight mode which is found only at the Bay of Konstanz station. This mode has an observed period of 14.6 minutes [9] compared to the predicted period of 14.3 minutes. It is evident from figure 7 that the waters of the Bay of Konstanz

Table 2. Theoretically predicted and observed amplitude and phase distributions for the fundamental mode at 10 stations around Lake Constance. Amplitudes are normalized to unity and phases to zero at Ludwigshafen.

	Theoretical		Observed											
	ampl. norm.	minutes after	2.8.67 ampl.	time	21.7.67 ampl.	time	25.6.67 ampl.	time	28.6.73 ampl.	time	16.7.73 ampl.	time	24.8.67 ampl.	time
Ludwigshafen	1.0	0	1.0	0	1.0	0	1.0	0	1.0	0	1.0	0	1.0	0
Unteruhldingen	0.44	− 0.07	0.46	4	0.5	0	0.458	− 1					0.47	6
Konstanz-Staad	0.313	0.15	0.35	5										
Konstanz-Jakobsbad	0.272	0.15					0.25	2						
Hagnau	0.162	− 0.2	0.18	− 10		0	0.16	8					0.18	7
Friedrichshafen	0.075	− 28											0.1	0
Romanshorn	0.067	28	0.31	− 16		19	0.08	22					0.18	20
Langenargen	0.162	− 27.7	0.14	− 23		27	0.16	10					0.22	− 27
Lindau	0.394	− 27.1	0.54	− 29	0.66	− 30	0.46	28	0.49	36	0.59	39	0.55	− 26
Hard	0.413	− 27.5												

co-oscillate with the open lake seiche of this frequency. In addition, there is a weaker co-oscillation in this bay of the tenth mode of period 12.0 minutes. Either of these oscillations may account for the remarkable observations of seiches of Schulthaiss in 1549 [15].
In summary, at least the form of the predicted gravitational seiches have been identified through direct observations. In each case, the predicted period has consistently been several percent less than the observed period which is considered to be attributed to frictional effects. The predicted amplitude and phase distribution of the fundamental seiche has been confirmed with a degree of certainty not often found in numerical modeling of lakes. Certain features of the higher order seiches have been verified on a more qualitative basis, in particular the resonant co-oscillation of the eight order seiche in the Bay of Konstanz.

3. The generation of seiches by atmospheric disturbances

3.1 *Theory*

In this part, a theory is outlined for the excitation of seiches by wind and pressure gradient forcing of arbitrary time history. Measured atmospheric variables are subsequently employed as driving functions for the model. Finally, the model predictions are compared with the observed seiche motions.
The mathematical model of general forced motion is as follows:

$$\frac{\partial u}{\partial t} - fv + g\frac{\partial \eta}{\partial x} = -\frac{\partial P_a}{\rho \partial x} + \frac{\tau_x}{\rho h} - \frac{\tau_{bx}}{\rho h}$$

$$\frac{\partial v}{\partial t} + fu + g\frac{\partial \eta}{\partial y} = -\frac{\partial P_a}{\rho \partial y} + \frac{\tau_y}{\rho h} - \frac{\tau_{by}}{\rho h}$$

$$\frac{\partial \eta}{\partial t} + \partial\frac{(hu)}{\partial x} + \partial\frac{(hv)}{\partial y} = 0$$

where the variables have the previous definitions with the addition of barometric pressure, P_a, water density ρ, wind stress components, τ_x and τ_y and bottom friction components, τ_{bx} and τ_{by}.
This problem is solved by the spectral method rather than by more traditional time-stepping techniques. This method exploits the linearity of the basic set of equation and has the advantage of computational efficiency, and allowing direct examination of the basic physics of the generation process. Thus, the relative importance of friction, pressure gradient and wind forcing may be readily investigated.

The spectral method

Suppose that spatial derivatives in the above equations are approximated by a treatment similar to that discussed in the seiche problem, then the resulting set of ordinary differential equations may be written in the matrix notation as

$$\frac{dM}{dt} = [A]M + T(t)$$

where the vector, M, now represents the unknown free surface displacements and current components at each nodal point; the vector, T, the wind stress and pressure gradients at each node, and the matrix, A, the matrix of coefficients or stiffness matrix which includes implicitly the factors, f, g, h and the parameterization of bottom friction. The precise form of these matrices need not be of concern at the moment.

The solution of the above matrix differential equation may be written formally as

$$M(t) = [X(t)]M(0) + \int_0^t [X(t-t')]T(t')\,dt'$$

where $X(t)$ is a combination of eigenvalues and eigenvectors of the matrix, A, and $M(0)$ is the initial state (Franklin [2]).

If we consider a simpler problem of a lake initially at rest which responds to a suddenly turned on wind stress of unit magnitude, it may readily be shown from the above general solution when the convolution integral is evaluated that the step function response may be written in the form

$$\eta(t) = SS + \sum_j^{n'} W_j\{C_j\}\, e^{i\sigma_j t}$$

where we have retained only the free surface displacement. SS is the steady-state solution and the second term on the right hand side is the weighted sum of the eigenvectors, C_j, oscillating with their characteristic frequencies, σ_j. In principle, the limit, n′, in the summation is the total number of eigenvectors contained in the coefficient matrix, A. However, a significant saving in computational effort may be effected if only the most important low order normal modes are used since it has already been observed in section 2 of this report that, in practice, only a small number of the possible free oscillations are excited in Lake Constance. Therefore, for the purposes of this calculation, we replace the limit, n′, by 11, the number of seiches calculated (m).

The problem remains of determining the unknown weighting coefficients, W_j, for each mode. Since the lake is initially at rest

$$-SS = \sum_{j=1}^{m} W_j C_j .$$

Also, the zero initial flow conditions yield

$$\left.\frac{\partial \eta}{\partial t}\right|_{t=0} = \left.\frac{\partial^2 \eta}{\partial t^2}\right|_{t=0} = 0$$

with the consequence that

$$i\sum_{j}^{m} W_j \sigma_j C_j = 0$$

and

$$-\sum_{j}^{m} W_j \sigma_j^2 C_j = 0.$$

If each nodal point is considered, there are, in general, many more equations than unknown weights in the case when only a few eigenvectors comprise the approximate solution. As a result, the weighting coefficients were found from the above conditions and by minimizing the square of the free surface deviation at each node in the lake. The method is the standard method of treating over-determined equations.

It may be noted that the general solution consists of a convolution integral form. Thus, in an analogous manner, we may write our general solution as a convolution of the time history of the wind stress and the barometric pressure gradient forcing with the approximate response function of the lake. Denoting the unit step function response of the lake to longitudinal wind stress as $\eta_{\tau x}$, the transverse wind unit stress response as $\eta_{\tau y}$ and similarly, for the unit pressure gradient responses resolved in the longitudinal and transverse directions, respectively, we may write the free surface displacement at any nodal point as

$$\eta(t) = \int_0^t \frac{d\eta_{\tau x}}{dt}(t-t')\tau_x(t')\,dt' + \int_0^t \frac{d\eta_{\tau y}}{dt}(t-t')\tau_y(t')\,dt'$$
$$+ \int_0^t \frac{d\eta_{px}}{dt}(t-t')\frac{\partial P_a}{\partial x}(t')\,dt' + \int_0^t \frac{d\eta_{py}}{dt}(t-t')\frac{\partial P_a}{\partial y}(t')\,dt' \qquad (1)$$

(see Hildebrand [5]).

Since the wind and pressure forcing function are usually not continuous functions but are known only at discrete intervals of time, the convolution in the discrete form is simply a digital filter of the form

$$\eta_k = \Delta t\left(\sum_{j=0}^{m} \frac{d\eta_{\tau_x}}{dt}\tau_{xk-j} + \cdots\right).$$

The upper limit in the expression, m, is specified at the point where the response becomes vanishingly small.

Up to this point no mention has been made of the determination of the steady-state solution, SS. In order to obtain this solution, we first decompose the steady free surface into a contribution from the wind stress alone. We resort to the solutions obtained by Welander [17] for the steady-state linearized equations of three-dimensional flow for the components of vertically integrated transport, U and V, as follows

$$U = \frac{1}{f\rho}(C\tau_x - D\tau_y) + \frac{gh}{f}\left(E\frac{\partial\eta}{\partial x} - F\frac{\partial\eta}{\partial y}\right),$$

$$V = \frac{1}{f\rho}(D\tau_x + C\tau_y) + \frac{gh}{f}\left(F\frac{\partial\eta}{\partial x} + E\frac{\partial\eta}{\partial y}\right).$$

Here, C, D, E and F are functions of the depth, the rotation rate and the vertical eddy viscosity as given by Welander [17].
The determination of the free surface distribution under a steady wind stress is most conveniently handled by the Galerkin formulation, whereby the vertically integrated equation of continuity is multiplied by a weighting function $W(x, y)$ and is integrated over the lake surface area to yield

$$\int\int W\left(\frac{\partial U}{\partial x} + \frac{\partial V}{\partial y}\right) dx\,dy = 0.$$

In this formulation, the weighting function, W, is identified with the Lagrangian interpolation function mentioned in section 2 in the seiche model.
After applying the Green's theorem on the plane, we have

$$\oint W(\vec{V}\cdot\vec{dn}) - \iint\left(U\frac{\partial W}{\partial x} + V\frac{\partial W}{\partial y}\right) dx\,dy = 0$$

where $\vec{dn}$ and $\vec{V}$ denote the vector of the line element directed normal to the boundary and the transport vector, respectively.
The line integral is zero in the case of Lake Constance when we ignore the contribution to the free surface due to river flow through. After eliminating the transports through Welander's solution the results may be expressed as

$$\iint gh\left(E\frac{\partial\eta}{\partial x} - F\frac{\partial\eta}{\partial y}\right)\frac{\partial W}{\partial x}dx\,dy + \iint gh\left(F\frac{\partial\eta}{\partial x} + E\frac{\partial\eta}{\partial y}\right)\frac{\partial W}{\partial y}dx\,dy$$

$$= -\iint [C\tau_x - D\tau_y]\frac{\partial W}{\rho\,\partial x}dx\,dy - \iint (D\tau_x + C\tau_y)\frac{\partial W}{\rho\,\partial y}dx\,dy.$$

When the integrations are performed in exactly the same fashion as in the case of seiche calculations element by element and the successive contributions added together a set of algebraic equations results of the matrix form

$$[A]\eta = B$$

which has been solved by standard methods. Here A is a square coefficient matrix and the vector B contains the forcing function. Theoretical water level set-up for the two components of wind stress are presented in figures 9 and 10. The associated circulation patterns are given in Hollan and Hamblin [7].
The other part of the steady-state solution stemming from the pressure gradient field is simply the water level distribution arising from the inverted barometer effect. For the purpose of the calculation, 1 cm of water was taken as equivalent to 1 mb of pressure.

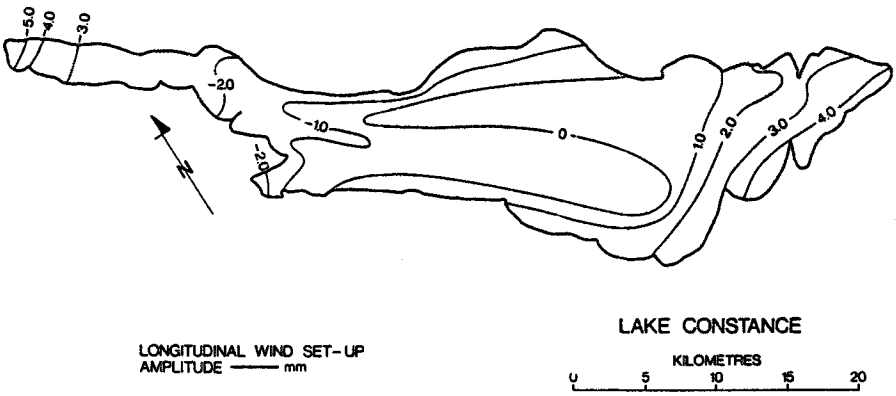

Figure 9. Water level set-up in cm for an eddy viscosity of 100 cm^2/s and wind stress of 1.0 $dynes/cm^2$ along the longitudinal axis of Lake Constance.

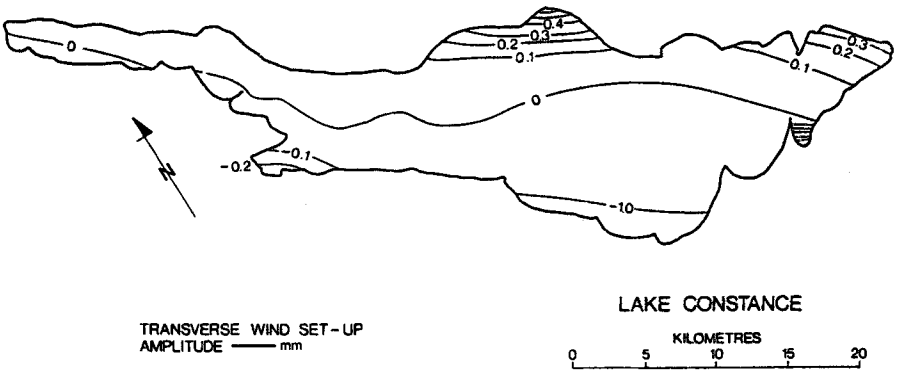

Figure 10. Water level set-up in cm for an eddy viscosity of 100 cm^2/s along the transverse axis of Lake Constance for unit wind stress, cgs.

3.2 *Frictional effects*

Before the weighting coefficient may be calculated, it is necessary to quantify the influence of friction. First, a number of numerical experiments of the effect of vertical eddy viscosity on the free surface demonstrated that the maximum set-up between the two ends of the lake is changed by only 10% by two orders of magnitude change in eddy viscosity which is in agreement with Welander's [17] results. For the purposes of the calculation of the wind-driven steady-state solution, a value of vertical eddy viscosity of 100 cm^2/s was adopted for the reason that it agrees with conventional specification of this parameter in lakes.

In the case of the seiches, the influence of friction is less well known since the theory at the present stage of development does not include the effect of friction. However, it has been established from observations that the factor, Q, in the expression for the damping of seiches

$$e^{-\frac{\sigma t}{2Q}}$$

(where σ is the inviscid frequency) varies from 40 to 50 for the fundamental longitudinal seiche of Lake Constance. Hollan [6] measured a Q of 45 from the seiche of 20 November 1972, while Forel [1] observed a case of probably 120 oscillations before the ultimate disappearance of the event, but that generally approximately 50 occurred. Therefore, we have adopted a Q of 40 in the calculation of the free surface response functions required by the spectral method on the basis of field observations.
In summary, the derivation of ingredients required in the convolution integral, equation (1), has been outlined. At the beginning of the computations, it is assumed that all water levels and currents are zero.

3.3 *Preparation of the data*

The network of 10 water level gauges, 5 barometric pressure stations and 16 wind measurement points established during the period of study have been described by Mühleisen and Fischer [9]. The sites of the observational stations used for the evaluation are included in figure 11. A number of episodes of pronounced seiche activity were selected on the basis of the availability of atmosphere records. Readings of wind speed, wind direction and barometric pressure were scaled manually from analogue recordings at intervals of one quarter of an hour. Wind stress, τ, was computed from the measured shoreline wind velocity, $\vec{V}$, using the aerodynamic drag formula with a drag coefficient, C_D, according to the expression

$$\tau = \rho_{air} C_D |\vec{V}| \vec{V} \tag{2}$$

where ρ_{air} is the density of air. The specification of the drag coefficient will be discussed shortly.
Wind stress components resolved along the longitudinal axis (300°) were then combined from two or more locations to form a lake-wide average. Similarly, the lake-wide averaged transverse wind stress was computed. Finally, averages at 7.5-minute intervals were obtained by linear interpolation between the 15- and 10-minute readings. The wind stations used in this calculation were considered to be representative of the over-lake wind field due to their favourable exposure at Lindau, Unteruhldingen and Romanshorn.
Barometric pressure readings were similarly scaled at either 15-minute intervals, 10-minute or 7.5-minute intervals depending on chart resolutions. To remove systematic variations between pressure stations, the average station pressure over the entire period of interest was removed from each series before the pressure gradients were calculated. As in the case of the wind stress field pressure gradients were obtained in the same longitudinal and transverse directions. Finally, gradients at 7.5-minute intervals were obtained by linear interpolation in time when necessary. Episodes varied in length for 24 to 48 hours depending on the duration of the storm and the availability of the data.

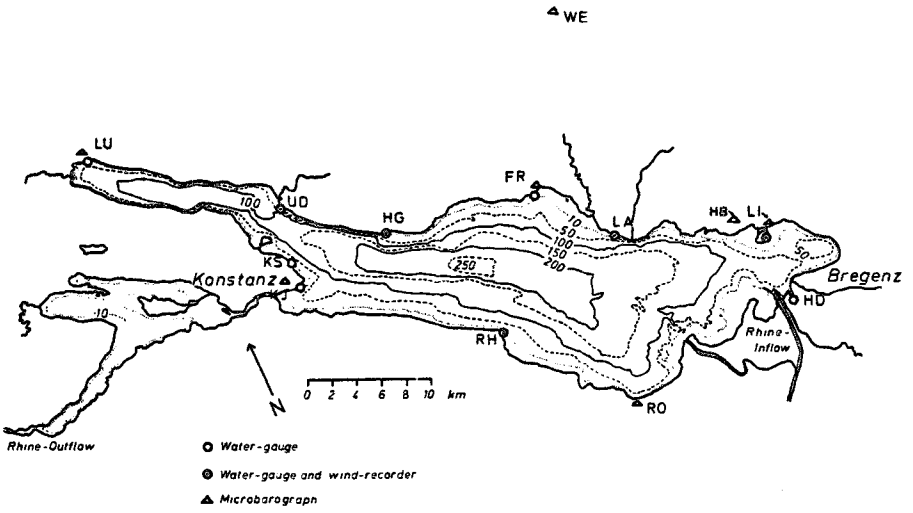

Figure 11. Bathymetry of Lake Constance and location of place names and observational stations used in the text and for evaluation. (Depths in meters, FR = Friedrichshafen, HD = Hard, HG = Hagnau, KJ = Konstanz-Jakobsbad, KS = Konstanz-Staad, LA = Langenargen, LI = Lindau, LU = Ludwigshafen, RH = Romanshorn, RO = Rorschach, WE = Weissenau, HB = Hoyerberg.)

3.4 *Results*

In all 10 cases studied, water level observations were available at the 2 principal stations along the longitudinal axis of the lake, Ludwigshafen and Lindau. Predictions at these 2 stations were scaled by means of the factor, C_D, in equation (2) to bring the predicted amplitudes of the water level fluctuations into general agreement with observed water levels. The apparent drag coefficients inferred by this method are listed in table 3.

Because of the limitations of space, results from only 5 of the 10 storms studied are displayed. In figure 12, one typical case from the years 1967 and 1973 is presented

Table 3. Observed peak wind speeds (m/s) and directions (deg from N), inferred drag coefficients, and ratio of pressure gradient contribution to wind contribution for the water level at Ludwigshafen and for ten examples of seiche generation, Lake Constance.

Episode	Ratio pressure/ wind at Ludwigshafen	$C_D \times 10^3$	Wind direction	Wind speed
18-19 June 1967	0.8	2	275	23
25-27 June 1967	1.2	6	290	9
21-23 July 1967	4.0	8	300	6
2- 3 August 1967	0.2	8	300	10
23-24 August 1967	0.2	6	180	8
27-29 June 1973	0.8	8	270	8
15-16 July 1973	1	4	280	13
9-10 September 1973	0.25	1.5	240	17
16-18 October 1973	0.2	2	270	18
14-15 December 1973	0.5	2	280	20

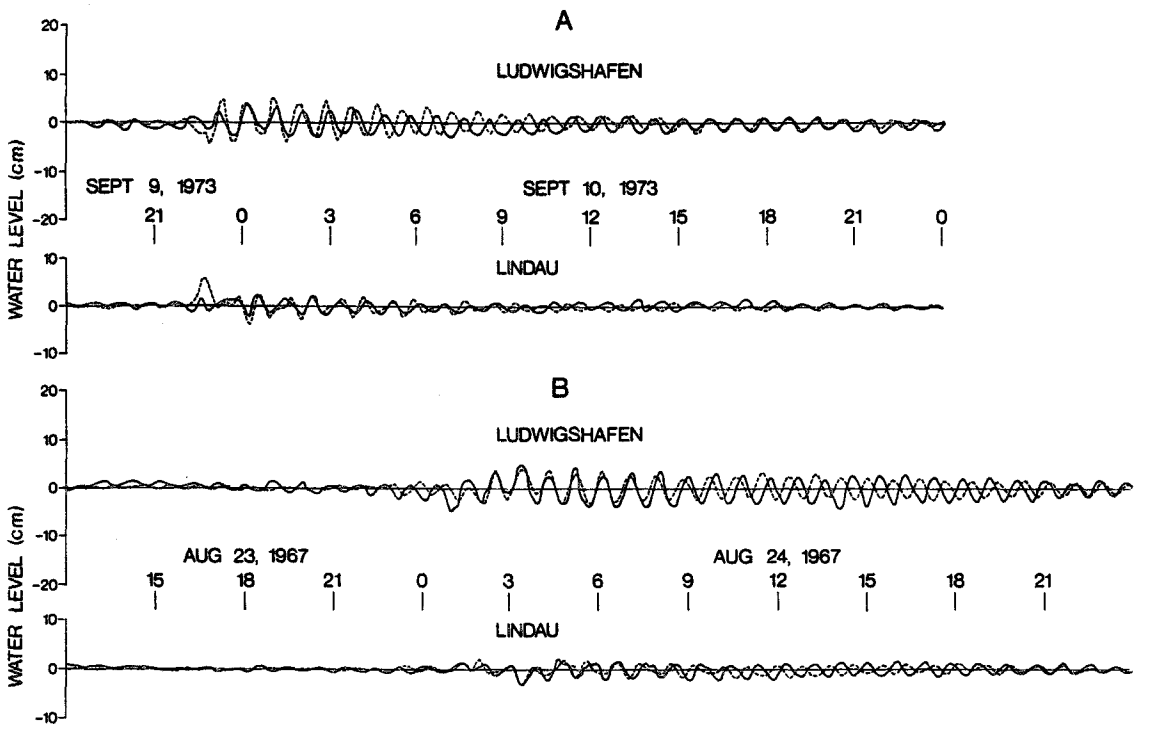

Figure 12. Predicted (- - - -) and observed (———) water levels at Ludwigshafen and at Lindau for a) 9–10 September 1973, b) 23–24 August 1967.

for the 2 principal stations while in figure 13, one example of a wind forced seiche and one example of a pressure forced seiche is depicted. Estimates of the relative contributions of wind and pressure forcing are given in table 3 by episode.
For about one-half of the cases studied, water level data were also available at locations other than at the ends of the lake. One example of the character of the seiches and the predicted response at transverse stations is provided in figure 14.

3.5 *Discussion*

Provided that the drag coefficient in equation (2) is adjusted from storm to storm, it is possible to predict water level fluctuations which are in reasonable agreement with the observations. At the onset of a storm, the agreement is usually best. Following this period, the predictions degrade for two reasons. After about 6 oscillations of the fundamental seiche, the predictions appear to be out of phase with the station data. Since the theoretical period of the fundamental seiche is 4% less than the observed after a number of periods of oscillation, the accumulated error accounts for this discrepancy. Secondly, the predicted amplitudes decay slightly more rapidly than the observed amplitudes. This suggests that our chosen value of

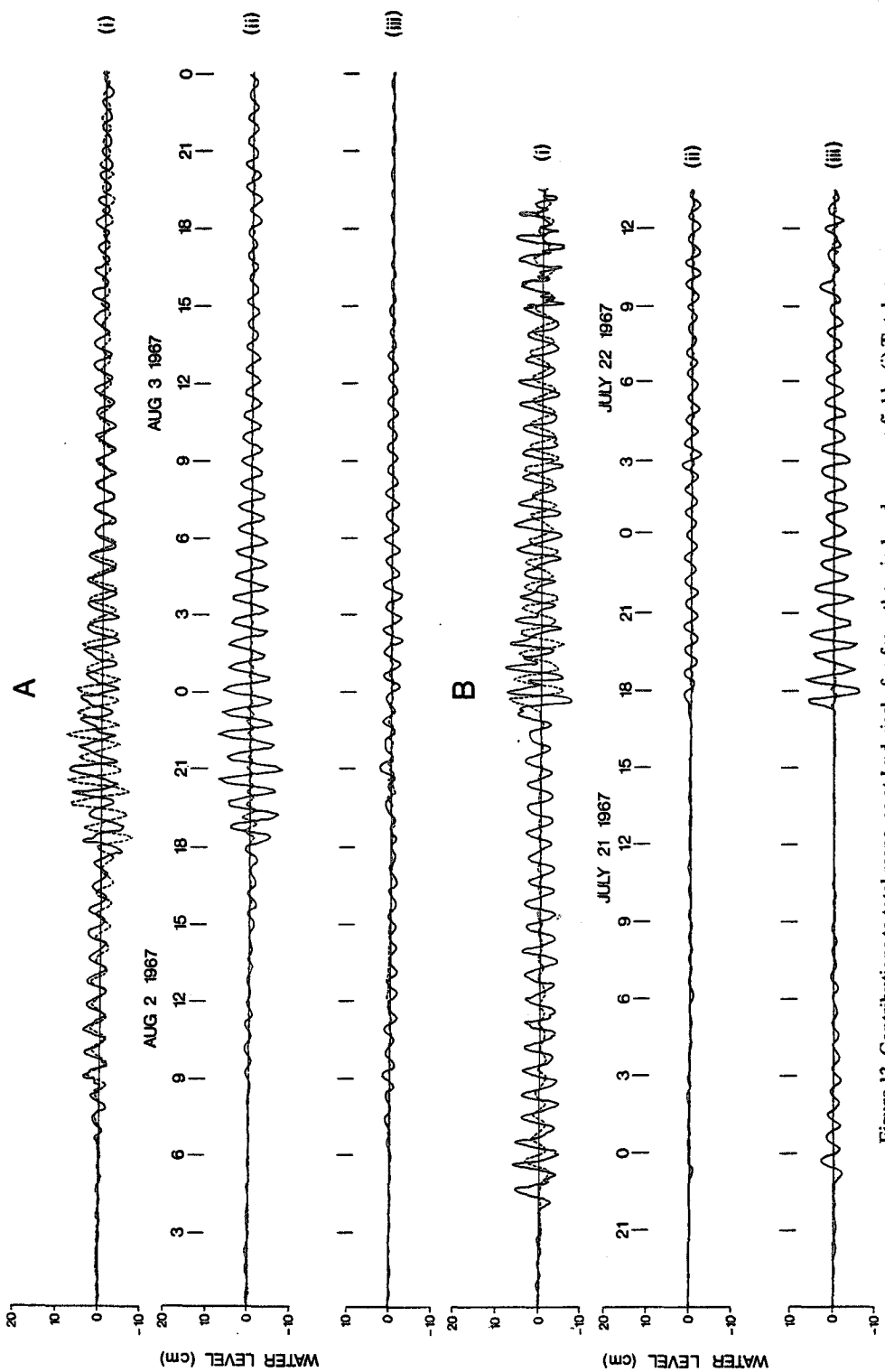

Figure 13. Contributions to total response at Ludwigshafen from the wind and pressure fields. (i) Total response, (———) observed, (- - - -) predicted; (ii) wind stress response only, (———) longitudinal, (- - - -) transverse component; (iii) pressure gradient component, (———) longitudinal, (- - - -) transverse. Panel A refers to the case 2–3 August 1967 while B is the case 21–22 July 1967.

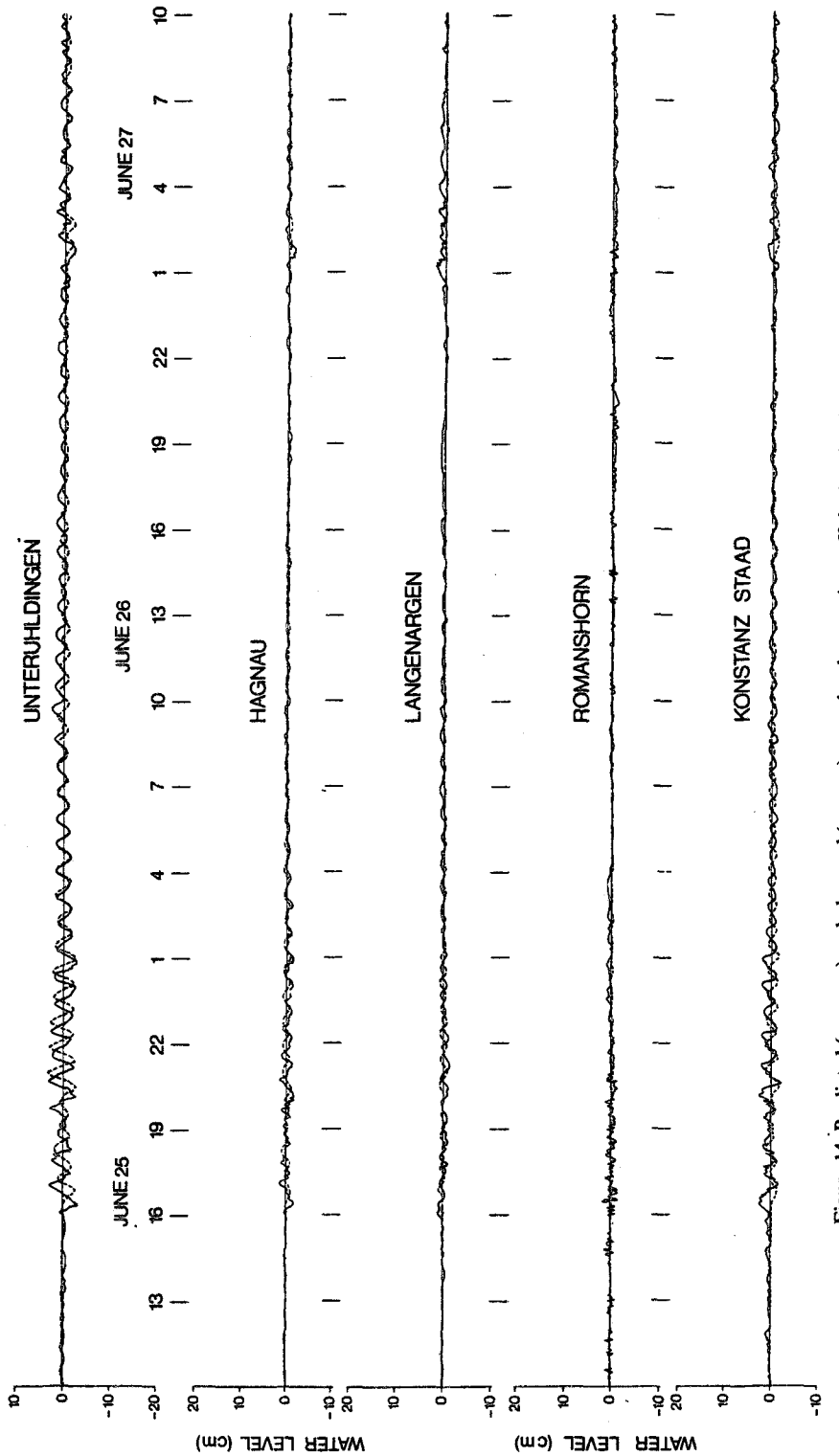

Figure 14. Predicted (- - - -) and observed (——) water levels at stations off the longitudinal axis of Lake Constance for the storm of 25–27 June 1967. Station locations are shown on figure 11.

the factor, Q, parameterizing the damping effect, is somewhat low. It was felt that this difference in Q is too small to warrant recalculation of the ten episodes.
Examination of figure 12 reveals that the amplitudes of the seiches at Ludwigshafen are predicted to be greater than those at Lindau and that the water level fluctuations are out of phase between the ends of the lake. These findings are in agreement with the observations.
At first sight, it may appear unreasonable to vary the drag coefficients by a factor of 4 or more from occasion to occasion. However, it may be recalled that the wind measurements were obtained from shore based stations. We postulate that the variation of the apparent drag coefficient embodies the square of the land-lake wind ratio and the true drag coefficient itself remains constant with a fixed value of 2×10^{-3}. For example, a drag coefficient of 8×10^{-3} implies an over-lake to land wind ratio of 2 providing that a conventional drag coefficient for high wind cases is assumed [16]. Studies of these ratios in the Great Lakes [13] yield wind ratios as high as 3 for low wind speeds and unstable atmospheric conditions, but are generally close to 2 for winds less than 8 m/s. They find also that the wind ratio approaches unity for high wind speed. Similarly, in Lake Constance, we remark in table 3 that wind ratios (drag coefficients) are lower under high peak wind conditions. Unfortunately, we do not have access to data required to estimate the effect of atmospheric stability for these cases but, nonetheless, classify the data into three groups; 1. peak wind of less than 10 m/s and wind ratios of 2.0; 2. peak wind over 15 m/s and wind ratio of 1.0; and 3. an intermediate class lying between the other two classes. Direct measurements of the wind ratios on the lake are rare. However, we may compare our findings with those of Mühleisen [11] who obtained wind ratios of 2 on three occasions.
The close agreement of the mathematically modelled seiching activity with the natural events establishes with certainty the meteorological causes of seiches in Lake Constance. From data presented in table 3 and in figure 13 on the separate contributions to the overall water level response from the barometric pressure field and from the wind stress field, it appears that wind forcing on the whole is more influential than is the pressure gradient. On the other hand, since Lake Constance is a relatively deep lake, barometric pressure influence may not be neglected and, at times, provides the dominant of generation of seiches. Examination of table 3 reveals that, in general, wind generation of seiches prevails during the spring and fall but that during the summer pressure effects play a predominant role.
Up to this point, we have considered primarily the generation of the fundamental mode of oscillation as exemplified by the response at stations located at the distal points of the lake. At locations in proximity to the node of the fundamental seiche, higher order normal modes are frequently observed. The predictions at these points shown on figure 14 agree less well with observations than do the results at the ends of the lake. It is not known whether or not these discrepancies arise from the poorer temporal resolution of the forcing fields relative to the period of the higher normal modes. In order to generate seiches of periods from 10 to 20 minutes, we require data of resolution superior to 15 minutes intervals. An additional source of uncertainty is the neglect in the modeling procedure of spatial variation of the wind and pressure fields. Due to the paucity of meteorological data further refinement

is not warranted at this time. An investigation of this problem of the contribution to the generation of seiches by spatial variation of the forcing field is conducted in Appendix I.

The analysis of Appendix I indicates that the spatial variation of the forcing field has a substantial influence on the excitation of seiches. Except for the deviations in the response caused by the irregular two-dimensional bathymetry, the results of the simple one-dimensional model are valid for the two-dimensional case of generation. The comparison of the response in the case of spatially varying forcing with the case of linearly interpolated uniform forcing yields the following results. If the speed of travel, v, of the assumed idealized disturbances is smaller than 0.5 c, where $c=31.32$ m/s is the mean phase speed of long waves in Lake Constance, a considerable increase of the response is associated with the interpolated forcing. For fast disturbances, $v>0.5$ c, the differences become smaller and vanish for very high speeds of travel. Thus the approximation of the spatial variation of the forcing fields applied in the two-dimensional calculations is only satisfactory in the range of high speeds of propagation. The analysis shows moreover, that the spatial variation of the driving forces generally cannot account for an alternative explanation of the large drag coefficients found by the comparison of predicted and observed generation of seiches.

4. Conclusions

It has been established that the problem of surface seiches in Lake Constance is amenable to modern hydrodynamical modeling techniques. These methods which treat the actual lake geometry and measured meteorological inputs in a realistic fashion are sufficiently accurate to allow certain conclusions to be drawn about such effects as the earth's rotation, friction, and the ratio of land winds to over-lake winds.

Because the seiches of Lake Constance occur in highly regular trains of oscillations, the periods may be estimated very accurately. Consistent underestimation of the observed periods by a few percent is thought to be due to the neglect of frictional and non-linear effects in the mathematical model of seiches. On the other hand, uncertainties as great as 5 minutes exist between stations so that the influence of the phase propogation of the seiche cannot be assessed. For example, we were not able to establish the predicted counterclockwise rotation of the fundamental mode. It is recommended for future studies of seiches that water level data with an absolute timing accuracy of 1 minute be recorded and that such statistical methods as spectral analysis be adopted.

Higher order seiches are less frequently observed in Lake Constance except perhaps at Romanshorn, Friedrichshafen, and the Bay of Konstanz where a remarkable co-oscillation exists with the eighth order seiche. At this location, our calculations confirm one of the earliest recorded observations of seiches by Schulthaiss [15].

The generation of seiches by wind stress and barometric pressure gradients has been established by the validation of 10 case histories of the excitation of seiches by field data. Winds are evidently more influential than pressure, but pressure effects may not be safely neglected on the whole. Predictions conform well to observations at

the ends of the lake but to a lesser degree at other points. It is recommended that more detailed measurements of the meteorological inputs both in time and space be taken to resolve these discrepancies.

An interpretation of the relatively high drag coefficient inferred in the study as the product of a conventional drag coefficient times the square of the lake-land wind ratio is consistent with the published studies of both these quantities in other lakes. Thus, the behaviour of the winds over the lake may be inferred. During the light winds, the wind field over the lake is twice as strong as that on the shoreline while for very strong winds, the difference vanishes. At this time, however, insufficient information exists on the spatial variation of forcing fields over Lake Constance to arrive at a satisfactory explanation.

In most instances, seiches are generated by rather sudden or impulsive changes in the strength and direction of the meteorological forcing field. Maximum seiche amplitudes are established after a few oscillations which are subsequently followed by a gradually decaying train of waves. Damping rates of seiches inferred from the model predictions agree closely with those obtained by simple visual inspection of the recordings. Frictional effects are evidently relatively weak as the fundamental seiche has an e-folding time of 13 periods.

Appendix I

In the two-dimensional model discussed thus far, the seiches are excited by a uniform spatial distribution of the external forces which are, in turn, only roughly approximated by linear interpolation between the observed data from a few stations on the shore. Since sufficient information does not exist on the real spatial distribution of wind stress and pressure disturbances over the lake, we may investigate this effect by means of idealized disturbances in a simple rectangular model of Lake Constance. According to Rossby [14], the radius of deformation, $r = c/f$, with the Coriolis parameter f and $c = \sqrt{g H}$, the phase speed of long waves, amounts to 291 km for the latitude and the mean depth of the lake. Since the greatest horizontal scale, the length of the lake is half a magnitude smaller than r, we may neglect for the present purpose the earth's rotation and the cross-lake components of motion. For a one-dimensional lake, the response of the normal modes to wind and pressure disturbances may be modeled by the following two systems of equations:

$$\frac{\partial^2 \varphi}{\partial t \partial x} = g \frac{\partial \eta}{\partial x} - \frac{\tau}{\rho H}, \qquad H \frac{\partial^2 \varphi}{\partial x^2} = \frac{\partial \eta}{\partial t}, \tag{3}$$

$$\frac{\partial \varphi}{\partial t} = g\eta + \frac{P_a}{\rho}, \qquad H \frac{\partial^2 \varphi}{\partial x^2} = \frac{\partial \eta}{\partial t}. \tag{4}$$

The displacement of the free surface is η, φ represents the velocity potential and τ and P_a the wind stress along the lake and the air pressure, respectively. The remaining quantities are the acceleration of the earth, g, the water depth, H, and the density of the water, ρ. The influence of friction is omitted, since it causes only a gradual exponential decay of the amplitudes and a small change in

the eigenperiods, which is unimportant here. The system (3) has been used in the same context by Rao [12], whereas the equations (4) are dealt with by Krauss [8]. It may be noted by the way, that the latter book contains a single differential equation for pressure-induced changes of the sea surface on p. 121, which are governed by the second derivative of P_a with respect to x. The corresponding solution is incomplete, because it does not contain the effect of spatially linear and constant pressure changes. The correct result is obtained, when the fundamental equations (4) are treated directly.
To solve for a rectangular lake, η and φ may be expanded in terms of the normal modes of the basin,

$$\cos \varkappa_m x$$

$$\eta = \sum_{m=1}^{\infty} \eta_m(t) \cos \varkappa_m x, \qquad \varphi = \sum_{m=1}^{\infty} \varphi_m(t) \cos \varkappa_m x, \tag{5}$$

with

$$\varkappa_m = \frac{m\pi}{L} = \frac{\sigma_m}{c}$$

where σ_m is the eigenfrequency of the m^{th} mode and $L = 62$ km is the length of the lake. For the depth, the mean value of 100 m is assumed.
Using equations (5) and the orthogonality properties of the normal modes

$$\int_0^L \cos \varkappa_m x \cos \varkappa_n x \, dx = \begin{cases} 0 & \text{for } m \neq n \\ L/2 & \text{for } m = n \end{cases}$$

the following inhomogeneous ordinary differential equations may be derived from equations (3) and (4)

$$\frac{d^2 \eta_m}{dt^2} + \sigma_m^2 \eta_m = -\frac{2\varkappa_m}{L\rho} \int_0^L \tau \sin \varkappa_m x \, dx, \tag{6}$$

$$\frac{d^2 \eta_m}{dt^2} + \sigma_m^2 \eta_m = -\frac{2H\varkappa_m^2}{L\rho} \int_0^L P_a \cos \varkappa_m x \, dx. \tag{7}$$

If the initial conditions, $d\eta_m/dt = \eta_m = 0$ at $t = 0$, are imposed and $f(t)$ denotes the inhomogeneous terms in the equations (6) and (7), respectively, the solution reads

$$\eta_m(t) = \frac{1}{\sigma_m} \int_0^t f(t') \sin \sigma_m (t - t') \, dt'. \tag{8}$$

A simple method of studying the effects of various spatial distributions of the generating forces is to consider the residual energy remaining in the oscillation once the disturbance has passed over the lake. This means that equation (8) has only to be evaluated for times, t, greater than the duration, T, of the disturbance over the lake.

In consideration of the pressure gradient forcing, a progressing front is assumed while for wind stress forcing a stress band is assumed since, in many instances of seiche activity, the forcing may be idealized by this type of excitation. For comparison, the response is determined from the interpolated distribution of forces when only the records of the assumed disturbances at 2 stations on the shore are known.

The transient region of the pressure front is defined by half a period of a sine function thus allowing for a steep or smooth type of front as the wave length, l, of the pressure change is varied. In addition, this front is allowed to travel at a constant speed, v, from west to east over the lake. The interpolated case is defined by linear interpolation between pressures at two locations along the length of the lake, d_1 and d_2. The complete definition of the 2 cases is listed and illustrated in table 4.

Similarly, the wind disturbance is defined in the same way. The stress band and the corresponding interpolated cases are given in table 5. The two types of forcing show considerable differences which are displayed in the table 5 by diagrams.

Solutions for η_m are obtained by straightforward integrations. First, the Fourier coefficients for τ and P_a have to be determined from equations (6) and (7). Then the convolution integral (8) has to be solved using these coefficients. The solution for $t \geq T$, the transition time of a disturbance, may be arranged into the form,

$$\eta_m(t) = \eta_{0,m} \cdot \sin\sigma_m(t - \Theta_m)$$

wherein the amplitude, $\eta_{0,m}$, contains the response of the normal mode in question and Θ_m is a constant which is generally different for each mode.

It is convenient to discuss the response in terms of the total energy per unit surface area for a standing wave, which is given by equation (9)

$$E_m = \frac{1}{4} g\rho\eta_{0,m}^2. \tag{9}$$

1. *Pressure gradient response*

For the case of the pressure front, the residual energy contained in mode m is

$$E_m = \frac{1}{g\rho}\left(\frac{4Aq}{m\pi(1-q^2)(1-m^2v^2q^2)}\right)^2 \cos^2\left(\frac{m\pi vq}{2}\right) \times \begin{cases} \sin^2\left(\frac{m\pi}{2}q\right), & m \text{ even} \\ \cos^2\left(\frac{m\pi}{2}q\right), & m \text{ odd} \end{cases}. \tag{10a}$$

Table 4. Definition of the temporal and spatial dependence of the pressure front and its corresponding distribution obtained by linear interpolation between two distant points on the shore.

t \ x	[o,vt]	[vt,L]			remarks
$\left[o,\frac{L}{2v}\right]$	$A\cdot\cos k(x-vt)$	A		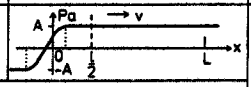	t=0, when the front enters the lake at x=0.
t \ x	$\left[o,vt-\frac{L}{2}\right]$	$\left[vt-\frac{L}{2},vt\right]$	[vt,L]		k=2π/L, v=const, speed of travel.
$\left[\frac{L}{2v},\frac{L}{v}\right]$	$-A$	$A\cdot\cos k(x-vt)$	A	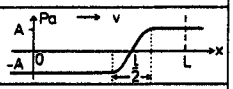	$T=\frac{1}{v}(L+\frac{L}{2})$, transition time.
t \ x	$\left[o,vt-\frac{L}{2}\right]$	$\left[vt-\frac{L}{2},L\right]$			
$\left[\frac{L}{v},\frac{L+\frac{L}{2}}{v}\right]$	$-A$	$A\cdot\cos k(x-vt)$		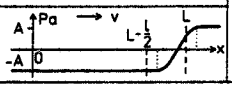	

t \ x	[o,d_1]	[d_1,d_2]	[d_2,L]		remarks
$\left[o,\frac{L}{2v}\right]$	$A\cdot\cos(kvt)$	$\frac{A}{d}[(x-d_1)+(d_2-x)\cos(kvt)]$	A	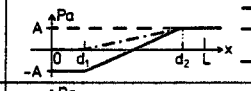	t=0, when the front arrives at x=d_1.
$\left[\frac{L}{2v},\frac{d}{v}\right]$	$-A$	$\frac{2A}{d}(x-d_1)-A$	A	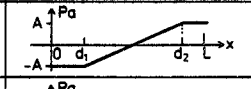	$d=d_2-d_1$, k and v as above.
$\left[\frac{d}{v},\frac{d+\frac{L}{2}}{v}\right]$	$-A$	$\frac{A}{d}[(x-d_2)+(x-d_1)\cos k(d-vt)]$	$A\cos k(vt-d)$	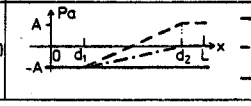	$T=\frac{1}{v}(d+\frac{L}{2})$, transition time.

Table 5. Definition of the temporal and spatial dependence of the wind stress band and its corresponding distribution obtained by linear interpolation between two distant points on the shore.

t \ x	[o,vt]	[vt,L]			remarks
$\left[o,\frac{L}{v}\right]$	F	0		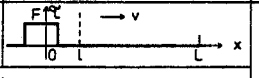	t=0, when the stress band enters the lake at x=0.
t \ x	[o,vt-l]	[vt-l,vt]	[vt,L]		v=const, speed of travel.
$\left[\frac{l}{v},\frac{L}{v}\right]$	0	F	0	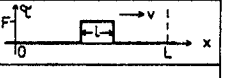	$T=\frac{1}{v}(L+l)$, transition time.
t \ x	[o,tv-l]	[vt-l,L]			
$\left[\frac{l}{v},\frac{L+l}{v}\right]$	0	F		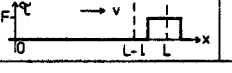	

t \ x	[o,d_1]	[d_1,d_2]	[d_2,L]		remarks
$\left[o,\frac{l}{v}\right]$	F	$-\frac{F}{d}(x-d_2)$	0	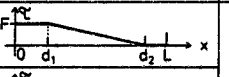	t=0, when the stress band arrives at x=d_1.
$\left[\frac{l}{v},\frac{d}{v}\right]$	0	0	0	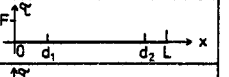	$d=d_2-d_1$, v as above, $T=\frac{1}{v}(d+l)$, transition time.
$\left[\frac{d}{v},\frac{d+l}{v}\right]$	0	$\frac{F}{d}(x-d_1)$	F	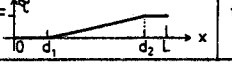	

In (10a) the ratios, $\nu = l/(2L)$ of the front width to the basin length, L, and $q = c/v$ the speed of wave propagation to the speed of travel of the front, are introduced. When $v = c$ and $v = m\nu c$ (10a) does not hold. By expanding numerator and the denominator in the neighbourhood of these arguments in a Taylor series, we obtain the following, for $v = c$

$$E_m = \frac{A^2}{g\rho(1-m^2\nu^2)^2}\cos^2\left(\frac{m\pi\nu}{2}\right) \quad \text{for all m} \tag{10b}$$

and for $v = m\nu c$

$$E_m = \frac{A^2\nu^2}{g\rho(1-m^2\nu^2)^2} \cdot \begin{cases} \sin^2\left(\frac{\pi}{2\nu}\right), & \text{m even} \\ \cos^2\left(\frac{\pi}{2\nu}\right), & \text{m odd} \end{cases} . \tag{10c}$$

In the case of the interpolated pressure disturbance, the result for $v \neq m\nu c$ will be for all m,

$$E_m = \frac{1}{g\rho}\left(\frac{8AL}{m^2\pi^2 d(1-m^2\nu^2q^2)}\right)^2 \sin^2\left(\frac{m\pi}{2L}(d_1+d_2)\right)$$
$$\times \sin^2\left(\frac{m\pi}{2}\frac{d}{L}\right)\cos^2\left(\frac{m\pi\nu q}{2}\right)\sin^2\left(\frac{m\pi dq}{2L}\right) \tag{11a}$$

with $d = d_2 - d_1$
and for $v = m\nu c$ for all m.

$$E_m = \frac{1}{g\rho}\left(\frac{2AL}{m^2\pi d}\right)^2 \sin^2\left(\frac{m\pi}{2L}(d_1+d_2)\right)\sin^2\left(\frac{m\pi}{2}\frac{d}{L}\right)\sin^2\left(\frac{\pi}{2\nu}\frac{d}{L}\right). \tag{11b}$$

Since the two-dimensional theory was primarily concerned with the excitation of the fundamental mode, it is sufficient to compare the residual energies for $m = 1$. For this purpose, equations (10) and (11) are evaluated in the range from $0.5 \leq q \leq 14$, for $A = 1$ mb and for $\nu = 0.01$. This means that the front consists of a pressure reduction of 2 mb in 620 m and is progressing with a speed in the range from $2.24 \text{ m/s} \leq v \leq 62.6$ m/s. In order to exhibit the influence of different positions of the stations, d_1 and d_2, 3 cases are considered.

1. Lindau-Ludwigshafen with $d_2 = 56$ km and $d_1 = 6$ km, respectively, designated by LILU;
2. Rorschach-Konstanz with $d_2 = 46$ km and $d_1 = 16$ km, respectively, designated by ROKN;
3. Lindau-Friedrichshafen with $d_2 = 57$ km and $d_1 = 38$ km, respectively, designated by LIFR.

The response of the fundamental mode due to a pressure front is displayed in figure 15 in terms of the total energy per unit area and of the amplitude, η_1, according to equation (9).

Contrary to the interpolated cases, the response to the frontal forcing diminishes generally as the speed of travel, v, decreases. At the lowest value, v=2.24 m/s, the reduction amounts to two orders of magnitude in energy and about one order in amplitude, whereas the response to the front prevails for fast speeds of travel (see, for example, at q=1 or v=31.32 m/s), but does not exceed 2.2 cm in amplitude.

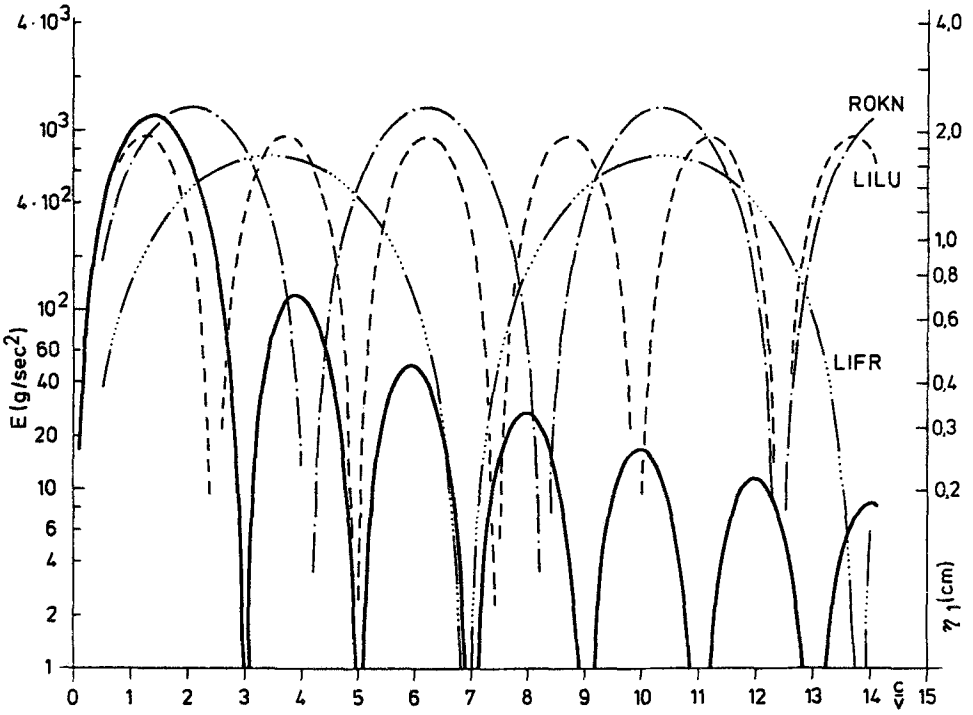

Figure 15. Response curves in terms of the energy, E, and of the amplitude, η_1, excited in the fundamental mode as function of the ratio of the gravitational wave speed, c, to the speed of travel of the pressure front, v. The labelled curves are explained in the text. The pressure front has a steepness of 2 mb/620 m.

The lobe-like nature of the response curves arises from the quenching effect of the oscillations. It is evident from inspection of the sine and cosine functions in equations (10) and (11) that the front excites the fundamental mode most effectively when the duration of each element of the front over the lake, $T_0 = L/v$, is a multiple of the fundamental period, $T_1 = 2L/c$, and that the oscillation is destroyed or quenched when the passage of elements takes an odd multiple n of half the fundamental period except for n=1.

For the interpolated cases, the peaks of the last sine function in (11a) occur at odd multiples of L/d and zeros at even multiples. According to this relation, the lobes become wider as the distance, d, between the stations decreases. This is clearly evident in the 3 cases shown in figure 15.
The principal difference between the response due to the front and that due to the interpolated cases becomes apparent when d approaches L. In this case, the oscillation is fully excited by the frontal disturbance, when that of the interpolated case is quenched.
With the help of the diagrams in table 4, the difference may be physically explained. Since the water surface follows immediately the pressure disturbance, it is obvious that the interpolated case for $d = L$ is most effective, when it lasts for an odd multiple of $T_1/2$ and has no effect for all whole multiples of T_1.
The response to the front may be explained only in a rough outline, because the convolution integral in the solution $\eta_1(t)$ according to equation (8) is more complicated. Greatest response will occur when the front is crossing the parts near the ends of the lake, where the greatest elevation of the oscillation takes place, in such a phase, when the directly forced displacement coincides with the vertical motion of the wave. At the western end where the front enters the lake, the water always follows in the same direction, as the pressure change requires it. A corresponding coincidence at the eastern end is, for example, only possible for $T_0 = T_1$. Then the surface is just rising by the induced oscillation, when the front is crossing and enforces the same direction of displacement. If T_0 amounts to whole multiples of T_1, the same conditions at the eastern end are met, but the central part of the basin contributes to a greater extent which reduces the response.
The first cosine factor in (10a) represents a modulation due to the time difference Δt between the transition time $T = T_0 + l/(2v)$ of the pressure disturbance and the duration, T_0, of its elements over the lake. Because of the narrow front ($l/2 = 620$ m) the speed of propagation of the disturbance must be very low in order to disclose the modulation. Since the range of evaluation with respect to q is not large enough, a detailed explanation is given in the context of the wind cases discussed below, for which longer disturbances are assumed and the influence of this modulation effect becomes more pronounced. For example, in figure 17, the complete modulation appears for the case of the longest wind disturbance.
A second evaluation of the pressure cases for a frontal width of 6.2 km ($\nu = 0.1$) does not yield substantial differences. The less steep front influences the response only for low transition speeds, v, as a consequence of the shorter modulation. For example, the residual energy of the secondary maximum at $q = 14$ amounts to 40% of the corresponding value in the case of $\nu = 0.01$. An evaluation of the solution in the range $0.1 < \nu \leq 1$ is presented by Mühleisen and Kurth [10].

2. *Wind stress response*

For the residual energy of the normal modes, the following expressions are obtained for excitation by the assumed wind disturbances. The response for the case of the wind stress band reads ($v \neq c$)

$$E_m = \frac{1}{g\rho}\left(\frac{4FL}{m^2\pi^2 H(1-q^2)}\right)^2 \sin^2\left(\frac{m\pi\nu q}{2}\right)\cdot \begin{cases} \sin^2\left(\frac{m\pi q}{2}\right), & \text{m even} \\ \cos^2\left(\frac{m\pi q}{2}\right), & \text{m odd} \end{cases} \tag{12a}$$

For $v = c$ the formula is valid,

$$E_m = \frac{1}{g\rho}\left(\frac{FL}{m\pi H}\right)^2 \sin^2\left(\frac{m\pi\nu}{2}\right), \quad \text{all m}. \tag{12b}$$

In the interpolated case, we have

$$E_m = \frac{1}{g\rho}\left(\frac{4FL}{m^2\pi^2 H}\right)^2 \sin^2\left(\frac{m\pi\nu q}{2}\right) \begin{cases} (1-B)^2\cdot\cos^2\left(\frac{m\pi}{2}\frac{d}{L}q\right), & \text{m even} \\ \left[(1-B^2)\cos^2\left(\frac{m\pi}{2}\frac{d}{L}q\right)+B^2\right], & \text{m odd} \end{cases} \tag{13}$$

where $B = \frac{L}{m\pi d}\left(\sin\left(m\pi\frac{d_2}{L}\right)-\sin\left(m\pi\frac{d_1}{L}\right)\right)$

and $d = d_2 - d_1$,

valid for all m.

The wind stress, F, is determined by the wind speed $\vec{V}$ in the x-direction at 10 m height above the surface according to equation (2) with a drag coefficient $c_D = 1.2\times 10^{-3}$. For a wind of 10^3 cm/s, the stress is approximately 1.5 g/(cm s^2). This value characterizes a moderately strong stress band and is used for the evaluation of two examples with different band widths; $l_1 = 6.2$ km and $l_2 = 12.4$ km corresponding to $\nu_1 = l_1/L = 0.1$ and $\nu_2 = 0.2$. The examples are treated in a similar manner to the pressure-induced responses. The complete definitions of the assumed wind disturbances are listed in table 5. In the interpolated case, three combinations of the stations, d_1 and d_2, are used in order to show the influence of different positions on the response. The following cases are selected.

1. Lindau-Unteruhldingen with $d_2 = 56$ km and $d_1 = 16$ km, respectively, designated by LIUN;
2. Langenargen-Unteruhldingen with $d_2 = 44$ km and $d_1 = 16$ km, respectively, designated by LAUN;
3. Langenargen-Lindau with $d_1 = 44$ km and $d_2 = 60$ km, respectively, designated by LALI.

The results for the response of the fundamental mode for $\nu = 0.1$ are displayed by the diagram in figure 16 while those for $\nu = 0.2$ are illustrated in figure 17.

At first sight, the general decay of the response to the stress bands with decreasing speed of travel and the low amount of energy excited in the range $0 \le q \le 14$ is striking. The highest peaks for the assumed wind field correspond to $\eta_1 = 0.8$ cm. If we examine the second factor in the brackets in the expressions (12) and (13),

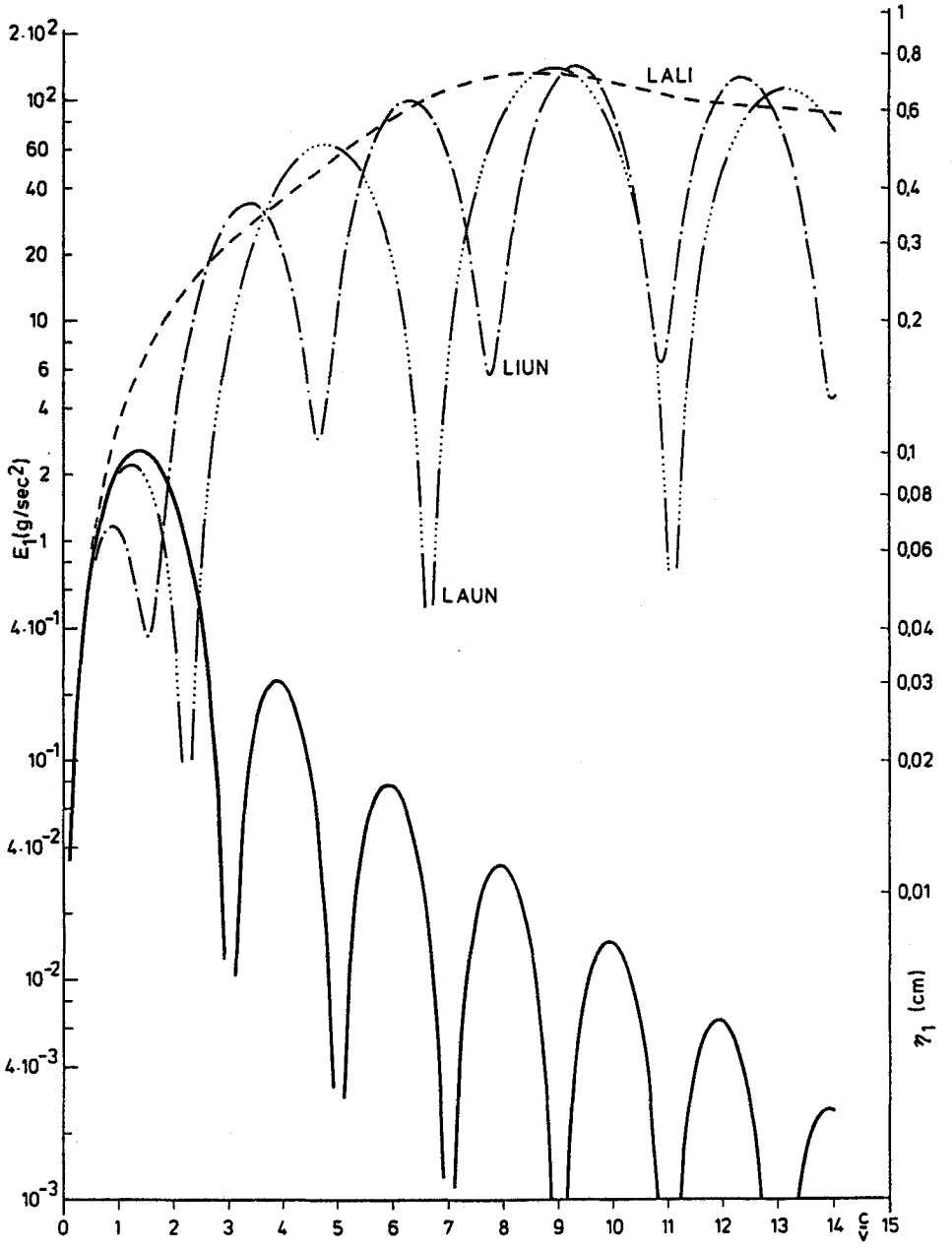

Figure 16. Response curves in terms of the energy, E, and of the amplitude, η_1, excited in the fundamental mode as a function of the ratio of the gravitational wave speed, c, to the speed of travel of the wind stress band, v, for a wind stress band of width 6.2 km. All curves are for a wind speed in the stress band of 10 m/s. Labelled curves are explained in the text.

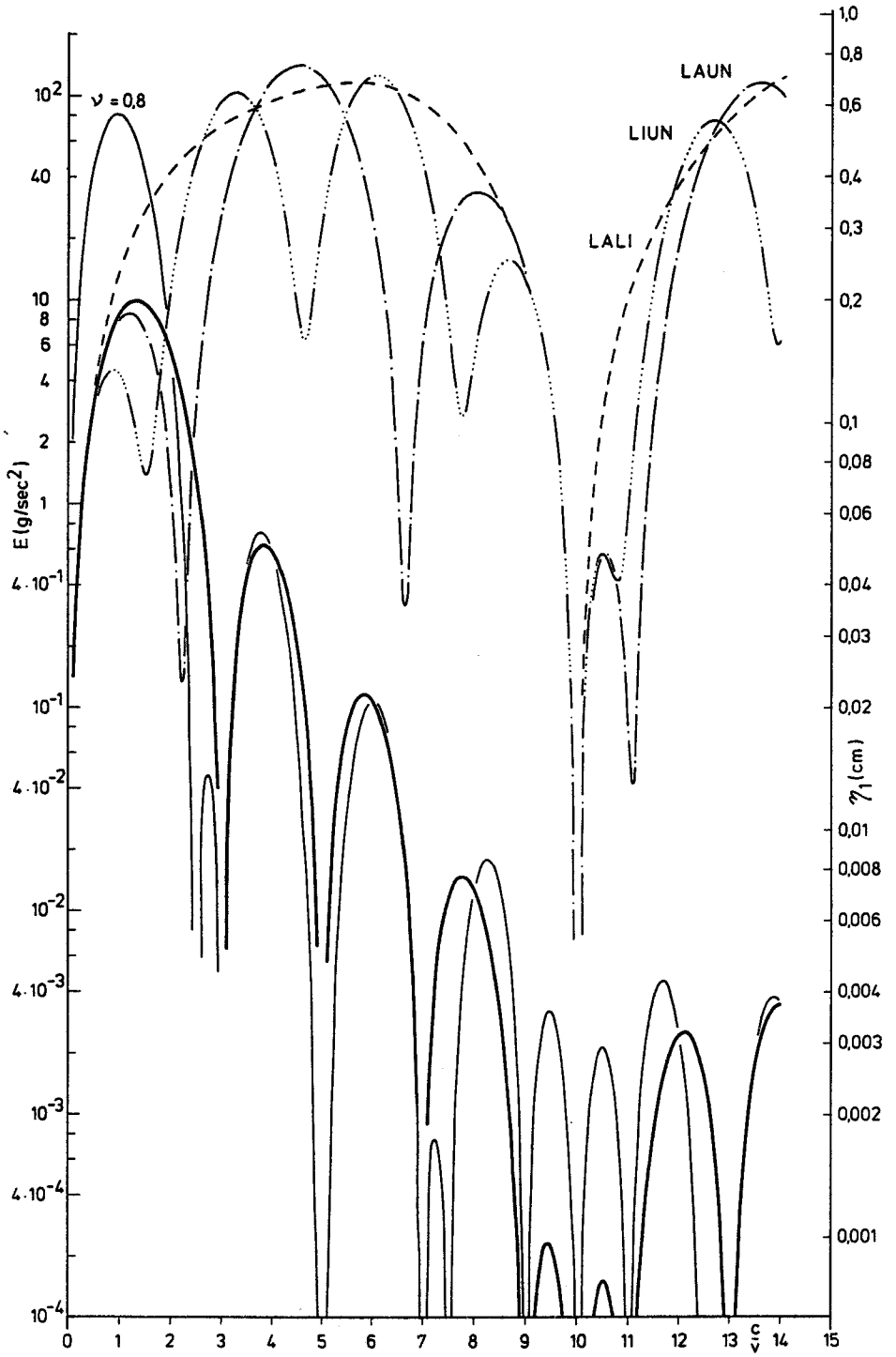

Figure 17. Response curves in terms of the energy, E, and of the amplitude, η_1, excited in the fundamental mode as a function of the ratio of the gravitational wave speed, c, to the speed of the stress band, v. All curves are for a wind speed of 10 m/s in the stress. The response for a wind stress band of width 12.4 km is depicted by the heavy line, whereas the response for a wind stress band of width 49.6 km ($\nu = 0.8$) is displayed by the light line. Labelled curves are explained in the text.

the dependency on the ratio L/H shows that more energy has to be supplied by the wind in a deep lake to excite a given amplitude than in a shallow lake. If we compare the peaks in figures 16 and 17 for the two stress bands in the range $0 \leq q \leq 3$, it is obvious that the residual energy has increased by doubling the width of the stress band. The increase of the response in the same range of q is about one order of magnitude in energy, if the width is approaching the length of the lake. A corresponding case for $\nu = 0.8$ is included in figure 17. According to the quadratic relation (2) between wind stress and wind speed the magnitude of the response is governed by the latter quantity. Since the assumed value, $V = 10$ m/s, is rather moderate and since the wind over the lake is known to be stronger than on the shore [11], a considerable increase of the residual energy has to be expected.

A more detailed discussion of the influence of spatial variation in the wind stress forces contained in the solutions (12) and (13) is warranted. If we compare the mean effect of the interpolation in both examples in figures 16 and 17, there is only agreement for fast disturbances in the range $q \leq 0.5$, which is physically reasonable. For $q > 1.5$ the differences become striking. At $q = 14$ the response to the interpolated wind field is more than four orders of magnitude higher in energy than in the case of the propagating stress band. The width of the lobes in the interpolated cases depends in the same way on the distance, d, between the 2 stations as in the interpolated pressure cases. But the peaks are located at even multiples of L/d because of the cosine function in the last factor of equation (13) for $m = 1$. The corresponding secondary minima occur at odd multiples of L/d and are greater than zero, which means that the modes of odd order are not fully quenched.

As to the lobes in the cases of the stress band the extrema are distributed in the same way as in the case of the pressure front, because the governing factor in equations (10a) and (12a), the last cosine function, is the same. Thus the previously given explanation of the maximum response and the quenching of the fundamental mode in terms of the travel time, T_0, of elements of the disturbance across the lake remains valid for the cases of the assumed wind stress bands.

As mentioned in the discussion of the pressure-induced response, the modulation of the lobes is more pronounced due to the larger band width, l. The expression, $\nu q/2$, in the argument of the modulation factor in equations (12a) and (13) may be interpreted as the ratio $Q_{\Delta t}$ of the time difference Δt between the transition time T and T_0 to the fundamental period, T_1. This becomes evident when T and T_0 are rearranged into the form $T = T_1(1+\nu)q/2$ and $T_0 = T_1 q/2$ with the use of $T_1 = 2L/c$. In terms of $Q_{\Delta t}$, the zeros of the modulation are given by $Q_{\Delta t} = 1, 2, 3 \ldots$ and the maxima by $Q_{\Delta t} = 1/2,\ 3/2,\ 5/2 \ldots$ Thus, the first zero of this type appears for the case $\nu = 0.2$ in figure 17 at $q = 10$. The modulation of the response to the broad wind stress band ($\nu = 0.8$) included in figure 17 shows zeros at $q = 2.5$ and greater values in steps of $\Delta q = 2.5$ as it corresponds to the greater ratio ν for that case.

The physical reason for the modulation may be attributed to the finite length of the disturbance. The successive action of the front may be characterized by the delay, Δt, between the incidence of the front and the rear part of the disturbance. The contribution of this effect to the convolution integral (8) for η_1 results in the modulation as a secondary lobe-type structure imposed on the principal lobes. With respect to the assumed stress bands the modulation causes maximum response for Δt equal

to odd multiples of half the fundamental period and zero response for whole multiples of the period. The corresponding values of q result from the relation $\Delta t = T_1 \nu q/2$.

If the response of a higher mode is considered instead of the fundamental, Δt has to be used in the form $\Delta t = T_m \cdot m \nu q/2$ where $T_m = 2L/(mc)$. Then the argument of the modulation factors in the cases of the pressure front and the wind stress band reads $\pi \Delta t/T_m$. This form shows that the above interpretation applies generally, if the corresponding eigenperiod, T_m, is introduced as reference period.

Finally, it may be pointed out that there is a different process of excitation in the pressure gradient case. It is evident in the next to last cosine factors in equations (10a) and (11a) that maximum energies are generated for Δt equal to integer multiples of T_m which is contrary to the wind cases. The different function of the modulation in the assumed pressure and wind disturbances becomes apparent when the variation in the response to a disturbance is considered as its width tends to zero. In the case of the pressure front, the disturbance is transformed into a step function and a finite value of the response is maintained by the zero argument in the cosine as expected. On the other hand, the wind disturbance vanishes when the width of the stress band goes to zero. Then no response is possible which is verified by the corresponding sine function in the expressions (12) and (13).

Summarizing the discussion it has to be noted that more energy is transmitted to the normal modes in the case of fast propagating wind stress bands than by a pressure jump travelling with the same speed, when the horizontal scale of the disturbance is extended. The mean magnitude of the pressure-induced oscillation depends primarily on the amount of the pressure jump. Therefore, the generation of seiches by wind is evidently more sensitive to the spatial distribution of the disturbance.

Summary

Predictions of several numerical hydrodynamical models of seiches, water level set-up, and the generation of seiches and set-up by barometric pressure gradients and surface winds are compared to water levels on Lake Constance recorded at 10 stations over a period of 8 years. Solutions for two-dimensional gravitational seiches are obtained from an expression minimizing the total energy. Of the lowest eleven modes, the periods of the first several modes have been identified in the records. An interesting resonance of the Bay of Konstanz with the eighth and tenth modes has been established.

A simple prediction scheme for the generation of seiches involves the convolution of horizontal averages of the measured wind stress and barometric pressure gradient components with the computed response functions for the individual stations. Comparison of computed seiches at the ends of the lake agree favourably with the field readings for ten episodes of seiching activity. Wind stress forcing is generally more important than pressure gradient generation especially in the spring and fall, but pressure effects may not be neglected. The frictional damping of seiches is evidently weak with an e-folding time slightly larger than 13 oscillations of the fundamental seiches.

In certain episodes, unexpectedly large drag coefficients may be explained by an acceleration of the wind field from the shore to the open lake. The inferred ratio of over-lake to land-based winds is two for peak wind speeds less than 10 m/s and approaches unity for winds larger than 15 m/s. Unfortunately, the field data are insufficiently detailed to prove this result at the present time.

ZUSAMMENFASSUNG

Mit Hilfe hydrodynamischer, numerischer Modelle werden die Seiches des Bodensee-Obersees und deren Erzeugung durch Luftdruckveränderungen und Windeinwirkung für verschiedene Schwingungsfälle aus dem Zeitraum 1966 bis 1973 berechnet, die durch Beobachtungsergebnisse von 10 Pegelstationen belegt sind. Die zweidimensionale Form und die Perioden der Seiches werden durch ein Variationsverfahren für die Energie freier Schwingungen des Sees erhalten. Von insgesamt elf berechneten Ordnungen der Seiches werden mehrere von niedriger Ordnung durch die Beobachtungsergebnisse verifiziert. Für die Konstanzer Bucht wurde eine Resonanz mit der achten und zehnten Eigenschwingung festgestellt.

Die Entstehung der Seiches wird mit einem einfachen Vorhersageverfahren untersucht, das auf der Faltung horizontal interpolierter beobachteter Windschubspannungen und Luftdruckgradienten mit den für die einzelnen Beobachtungsstationen berechneten Response-Funktionen beruht. Der Vergleich der berechneten Seiches mit den an den See-Enden beobachteten Schwankungen aus zehn verschiedenen Schwingungsfällen ergibt eine gute Übereinstimmung. Die Erzeugung durch Windeinwirkung ist im allgemeinen stärker ausgebildet, besonders im Frühjahr und Herbst; die Anregung durch Luftdruckschwankungen kann jedoch nicht vernachlässigt werden. Eine Abschätzung anhand der Beobachtungen zeigt ausserdem, dass die Schwingungen verhältnismässig schwach gedämpft sind. Für die Grundschwingung mit der berechneten Periode von 53,4 Minuten ergibt sich eine Abklingzeit auf 1/e der Anfangsamplitude von etwa 13 Perioden.

In einigen der zum Vergleich herangezogenen Schwingungsfälle müssen unerwartet hohe Schubspannungskoeffizienten angenommen werden, um Beobachtung und Rechnung in Deckung zu bringen. Die Ursachen hierfür sind in der Zunahme der Windgeschwindigkeit über dem freien See zu suchen. Es ergibt sich, dass die Windgeschwindigkeit auf dem freien See doppelt so gross ist wie am Ufer, wenn Spitzengeschwindigkeiten von 10 m/s nicht überschritten werden. Das Verhältnis ist eins für Spitzenwindgeschwindigkeiten grösser als 15 m/s. Das verfügbare Datenmaterial reicht nicht aus, um dieses Ergebnis durch Beobachtungen zu belegen.

RÉSUMÉ

Les prévisions de plusieurs modèles numériques hydrodynamiques de seiches, les montées du niveau d'eau dues au vent, la formation de seiches, les montées de niveau par gradients de pression barométrique et les vents de surface sont comparés aux niveaux d'eau du lac de Constance relevés dans 10 stations, sur une période de 8 ans. Les solutions aux seiches gravitationnelles à deux dimensions sont obtenues au moyen d'une expression réduisant l'énergie total au minimum. Des onze modes les plus bas, les périodes des quelques premiers modes ont été inscrites dans des relevés. Dans le cas de la baie de Constance, on a déterminé une résonance intéressante avec le huitième et le dixième mode.

Un système simple de prévision de la formation de seiches comprend la convolution des moyennes horizontales des efforts du vent mesurés et des éléments de gradients de pression barométrique avec les activités de réponse calculées pour chaque station. La comparaison des seiches calculées aux extrémités du lac s'accordent favorablement avec les relevés sur le terrain pour dix épisodes d'activité créant une seiche. La force d'entraînement, exercée par le vent est généralement plus importante que la formation du gradient de pression, surtout au printemps et en automne, mais on ne peut pas négliger les effets de la pression. L'amortissement des seiches par frottement est évidemment peu prononcé, et la durée d'enroulement est légèrement plus longue que celle de la seiche type qui comprend 13 oscillations.

Au cours de certains épisodes, on obtient des coefficients de résistance soudainement plus importants et qu'on pourrait expliquer par l'accélération du champ du vent, du rivage au lac exposé au vent. La différence entre les taux de vitesse du vent de terre et du vent passant au-dessus du lac est de

deux pour des vitesses de vent maximale de moins de 10 mètres à la seconde et s'approche de l'unité dans le cas de vents dont la vitesse est de plus de 15 mètres à la seconde. Les données obtenues sur place ne sont pas assez détaillées pour justifier ce résultat par des observations.

ACKNOWLEDGMENTS

The authors would like to express their gratitude to R. Mühleisen and his associates who kindly provided the material on which this study is based. The programme of observation was granted by the German Research Association. H. Helwig and W. Negel assisted with the data reduction. The evaluation of the theoretical results presented in the appendix has been carried out by J. Schwarz. Mrs. U. Zmudzinski from the Institute for Environmental Protection in Karlsruhe drew the figures and tables of the appendix and improved the representation of two preceding figures. Finally, C.H. Mortimer must be thanked for his encouragement to both authors in this study. The investigation was sponsored by the Canada Centre for Inland Waters and the Institute for Environmental Protection of the State of Baden-Württemberg as part of the bilateral agreement between the Canadian and the West German governments on scientific and technological collaboration of 1971.

REFERENCES

1 Forel, F.A.: Die Schwankungen des Bodensees. Schr. Verein. Gesch. Bodensees *22*, 49-77 (1893).
2 Franklin, J.N.: Matrix Theory. Prentice-Hall, Englewood Cliffs. N.J., USA. 1968.
3 Gasser, O.: Die Wasserspiegelschwankungen des Bodensees und ihre meteorologischen Grundlagen. Ber. D. Wetterd., No. 35 (vol. 5), 24 p., Bad Kissingen 1957.
4 Hamblin, P.F.: Some free oscillations of a rotating natural basin. Unpublished Ph.D. thesis. University of Washington, Seattle, USA, 1972.
5 Hildebrand, F.B.: Advanced Calculus for Applications. Prentice-Hall, Englewood Cliffs, N.J., USA, 1963.
6 Hollan, E.: Erste Ergebnisse des Strömungs- und Temperaturmessprogrammes im Bodensee 1972. Unpublished report. Institut für Meereskunde an der Universität Kiel, 1974.
7 Hollan, E., and Hamblin, P.F. (in German): Data Report on seiches, currents and circulation-calculations of Lake Constance, in preparation (1980).
8 Krauss, W.: Methods and Results of Theoretical Oceanography, vol. I, 302 p., Berlin 1973.
9 Mühleisen, R., and Fischer, A.R.: Über die Eigenschwingungen des Bodensees und ihre Anregung, 135 p. Unpublished report. Institute for Astronomy at the University of Tübingen, 1973.
10 Mühleisen, R., and Kurth, W.: Experimental investigations on the seiches of Lake Constance. Submitted to Schweiz. Z. Hydrol. *40* (1978).
11 Mühleisen, R.: Starkwinde an und auf dem Bodensee. Met. Rdsch. *30*, 15-22 (1977).
12 Rao, D.B.: Response of a Lake to a Time Dependent Wind Stress. J. Geophys. Res. *72*, No. 6, 1697-1708 (1967).
13 Richards, T.L., Drayert, H., and McIntyre, D.R.: Influence of atmospheric stability and overwater fetch on winds over the Lower Great Lakes. Mon. Weath. Rev. *94*, No. 7, 448-453 (1966).
14 Rossby, C.G.: On the mutual adjustment of pressure and velocity distributions in certain simple current systems. J. Marine Res. *1*, 15-28, 239-263 (1937).
15 Schulthaiss, Chr.: Wunder anloffen des Wassers. Collectaneen, vol. VI, p. 80½-81. Archive of the city of Constance, AI8 (1549).
16 Smith, S.D., and Banke, E.G.: Variation of the sea surface drag coefficient with wind speed. Quart. J.R. Met. Soc. *101*, 665-673 (1975).
17 Welander, P.: Wind action in a shallow sea: Some generalizations of Ekman's theory. Tellus *9*, 45-52 (1957).
18 Graf Zeppelin, E.: Die hydrographischen Verhältnisse des Bodensees, Bodensee-Forschungen, Teil III. Schr. Verein. Gesch. Bodensees *22*, Suppl., 61-103 (1893).

Addresses of the authors: Dr. Paul F. Hamblin, Canada Centre for Inland Waters, 867 Lakeshore Road, P.O.B. 5050, Burlington, Ontario, L7R4A6, Canada - Dr. Eckard Hollan, Landesanstalt für Umweltschutz Baden-Württemberg, Griesbachstrasse 3, Postfach 211310, D-7500 Karlsruhe 21, Bundesrepublik Deutschland.